Laga, University Paris 13

Master Internship Report

Mathematical modeling of biofilms resistance to antimicrobial agents

Author:
Dinh Anh Thi

Supervisor:
Prof. Linda El Alaoui

August 14, 2013

Mathematical modeling of biofilms resistance to antimicrobial agents

Master internship report

DINH Anh Thi
(dinhanhthimail@gmail.com)
Supervisor: Prof. Linda El ALAOUI
(elalaoui@math.univ-paris13.fr)
LAGA University Paris 13

August 14, 2013

Acknowledgements

First and foremost I offer my sincerest gratitude to my supervisor, Professor Linda El Alaoui, who has supported me throughout my thesis with her patience and knowledge. Without her, I cannot finish this internship in the convenient way. One simply could not wish for a better or friendlier supervisor.

During 3,5 months living and working in France, I am grateful to enthusiastic help of Professor Pascal OMNES, Mr. NGUYEN Van Tien. With their help, I got used to my new life very quickly.

I would also like to thank the staff of the LAGA laboratory for creating favorable conditions for me to work and study there.

Finally, I wish to thank my parents for their support and encouragement throughout my study.

Abstract

Almost all moist surfaces are colonized by microbial biofilms. A biofilm is a community of microorganisms (bacteria, fungi,algae and protozoa), adhering each other on a surface. Biofilms are, generally, observed in aqueous media or in a media exposed to moisture. They can grow on any type of natural or artificial surface. This surface may be mineral (rock interfaces, air-liquid ...) or organic (skin, plants), industrial (pipes, oil, waste water) or medical (prothesis, catheters),... (See more details in Section 1.1)

The presence of biofilms in a wide range of situations has led the researchers to study their properties both for their beneficial and detrimental impact. Biofilm bacteria show much greater resistance to antibiotics than their free-living counterparts and our interest here is to study the phenotypic reason of this resistance.

Neither reaction-diffusion limitation nor heterogeneities in growth-rate explain the observed tolerance. Another hypothesis is that specialized "persister" cells, which are extremely tolerant of antimicrobials, are the source of resistance. In this research, we want to investigate the effect of the reversion of persister cells to susceptible cells on the dosing of the antimicrobial agents.

It turns out that mathematical modeling can be an efficient tool for the study of biofilms. With this aim, we consider the model introduced in Chapter 3 in which the bacterial biofilm evolves in presence of a single nutrient (e.g. oxygen), a single antimicrobial agent and a neutralizing agent which reacts with the antimicrobial.

By using the finite element method, we perform the model by a finite element scheme. The obtained results via numerical simulations are used to propose a strategy for optimizing the antimicrobial dosing.

Key words: Biofilm, persister, susceptible, antimicrobial, resistance, dosing

Contents

List of Figures

List of Tables

List of notations

Differential Operators

$(x_1, ..., x_d)$	Cartesian coordinates in $\mathbb{R}^d$
$d_t u$ or $\partial_t u$	Time derivative of u
$\partial_i u$	Distributional derivative of u with respect to x_i
$\partial_{ij} u$	Second-order derivative of u with respect to x_i and x_j
∇u	Gradient of u: $\nabla u = (\partial_1 u, ...\partial_d u)^T \in \mathbb{R}^d$ if u is $\mathbb{R}$-valued or $\nabla u = (\partial_j u_i)_{1\leq i\leq m, 1\leq j\leq d} \in \mathbb{R}^{m,d}$ if u is R^m-valued
$\nabla \cdot u$	Divergence of u: $\nabla \cdot u = \Sigma_{i=1}^d \partial_i u$ if u is $\mathbb{R}^d$-valued or $\nabla \cdot u = (\Sigma_{j=1}^d \partial_j u_{ij})_{1\leq i\leq m}^T \in \mathbb{R}^m$ if u is $\mathbb{R}^{m,d}$-valued
$\beta \cdot \nabla u$	Advection operator: β is $\mathbb{R}^d$-valued and $\beta \cdot \nabla u = \Sigma_{i=1}^d \beta_i \partial_i u$
Δu	Laplace operator: $\Delta u = \Sigma_{i=1}^d \partial_{ii} u$ if u is $\mathbb{R}$-valued or $\Delta u = (\Sigma_{j=1}^d \partial_{jj} u_i)_{1\leq i\leq m}^T \in \mathbb{R}^m$ if $u$is $\mathbb{R}^m$-valued

Function Spaces

X'	Topology dual of topological space X
$\|u\|_X$	Norm of u in the norm space X
$\mathbb{P}_k$	Vector space of polynomials in the variables $x_1, ..., x_d$ of global degree at most k
$L^p(\Omega)$	Functions whose p-th power is Lebesgue integrable on Ω
$\mathcal{D}(\Omega)$	Infinitely differentiable functions compactly supported in Ω
$W^{s,p}(\Omega)$	Functions whose derivatives up to order s are in $L^p(\Omega)$
$W_0^{s,p}(\Omega)$	Closure of $\mathcal{D}(\Omega)$ in $W^{s,p}(\Omega)$
$\|u\|_{0,p}$	Norm in $L^p(\Omega)$: $\|u\|_{0,p} = (\int_\Omega \|u\|^p)^{\frac{1}{p}}$
$\|u\|_0$	Norm in $L^2(\Omega)$
$H^s(\Omega), H_0^s(\Omega)$	$W^{s,2}(\Omega), W_0^{s,2}(\Omega)$
$\langle u, v\rangle_0$	Scalar product on $L^2(\Omega)$: $\langle u, v\rangle_0 = \int_\Omega uv$
$L^p(]0, T[; V)$	V-valued functions whose norm in V is in $L^p(]0, T[)$

Chapter 1

Introduction

1.1 What is a biofilm?

You may be strange to the term "biofilm" but it is something that you may contact to everyday. The plaque that forms on your teeth and causes tooth decay and periodontal disease is a type of biofilm. Biofilm is simply defined as a community of micro-organisms (bacteria, fungi, algae and protozoa) attached to a surface. One more full definition of biofilm is "a layer of prokaryotic and eukaryotic cells anchored to a substratum surface and embedded in an organic matrix of biological origin", [13].

Biofilms are, generally, observed in aqueous media or in a media exposed to moisture. They can grow on any type of natural or artificial surface. This surface may be mineral (rock interfaces, air-liquid,...) or organic (skin, plants,...), industrial (pipes, oil, waste-water,...) or medical (prothesis, catheters,...),...

The life circle of a biofilm form can be described via three main stages: attachment, growth and dispersal [11, 7] (see Figure 1.1). In first stage, free-floating, or isolated planktonic-state microbes encounter a submerged surface and within minutes can become attached to this surface. They start to produce viscous extracellular polymeric substances (EPS) and to colonize the surface. In the second stage, EPS production allows the emerging biofilm community to develop a complex, three-dimensional structure that is influenced by a variety of environmental factors. Biofilm communities can develop within hours. Biofilm can growth under everywhere and conditions, things they need to growth may be mentioned as microorganisms, moisture, nutrients and surfaces [7]. Finally, the fully mature biofilm reaches a quasi-steady state where growth is balanced by loss through erosion and detachment due to mechanical stress. They can propagate through detachment of small or large clumps of cells, or by a type of "seeding dispersal" that releases individual cells. Either type of detachment allows bacteria to attach to a surface or to a biofilm downstream of the original community.

Are biofilms bad or good for human life? They are in both ways. We have talked about tooth decay above and there is also a link between biofilms with ulcerative colitis and several hospital acquired infections. To dentists and doctors, biofilms are more than an eyesore.

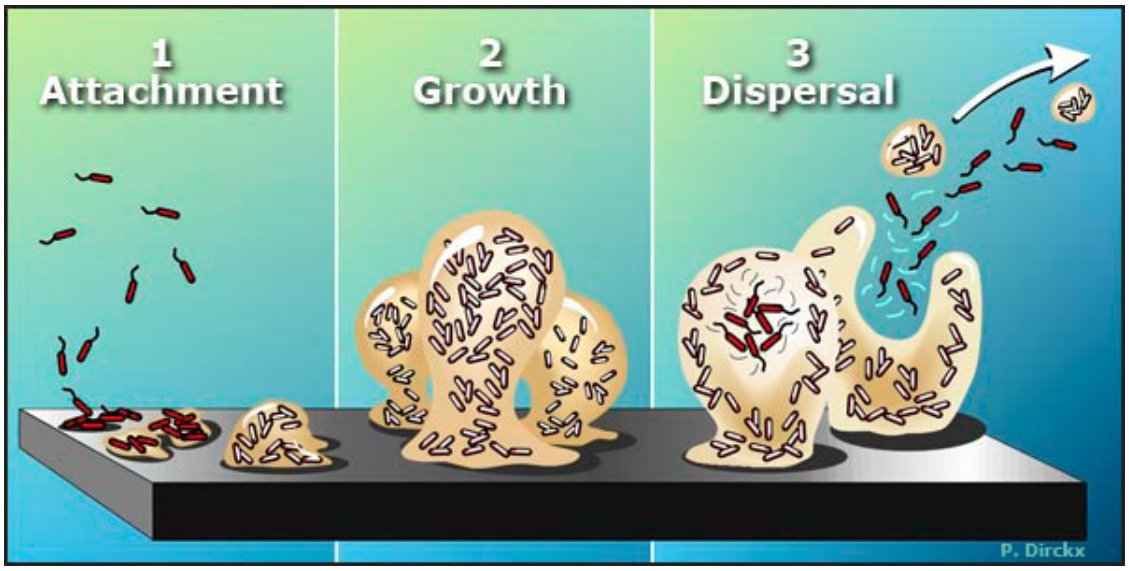

Figure 1.1: Stages of the biofilm life cycle, courtesy of the Montana State University Center for Biofilm Engineering, P. Dirckx.

They are expensive, destructive and sometimes deadly [8, 13]... Nevertheless, there are some good news in that not all biofilms are bad. Some industries use them in water-filter, production of medicines, food additives and even as cleaning agents [7, 13].

In this paper, we focus only on bad effect of biofilms in resistance to antimicrobial agents.

1.2 Resistance mechanisms of biofilm

As in Cogan's researches [6, 4], there are several hypotheses concerning resistance mechanisms of biofilms to antimicrobial. They are transport limitation, physiological tolerance and phenotypic resistance.

The first mechanism is the inability of the antimicrobial agent to fully penetrate the biofilm region. It is explained that penetration failure is due to a neutralizing reaction between the antimicrobial agent and some components of the biofilm. However, reaction limitation cannot completely explain biofilm resistance, since for antimicrobial agents that are not reactive or for thin biofilms where full penetration can be shown, susceptibility is still reduced substantially.

Another mechanism is physiological resistance. If the bacteria within the biofilm are not respiring, susceptibility to antimicrobial agents is typically decreased because most biocides and antibiotics are more effective at killing respiring bacteria than non-respiring ones. That is the reason why only the respiring fraction of bacteria are susceptible to killing. However, this mechanism cannot fully explain lowered susceptibility because if the nutrient can penetrate deeply into biofilm region or the time to be exposed is long enough, the bacteria can be eradicated completely. This is typically not the case in experimental studies. Therefore, other resistance must be explored. That is phenotypic resistance. In this type of resistance,

there exists "persister cells" which are extremely tolerant of antibiotics.

Our main interest here is to study the effect of the reversion of persister cells to susceptible cells on the dosing of the antimicrobial agents.

1.3 What is a mathematical model?

A mathematical model is a description of a system using mathematical concepts and language. The process of developing a mathematical model is termed mathematical modelling. In this work we develop a mathematical model describing the resistance of bacteria to antimicrobial agent. A good-understanding of this phenomenon is in accordance with a good model and inversely. Using and creating a mathematical model requires six steps:

1. *The important variables and processes acting in the system must be identified.* In our problem, necessary variables are substrate, antimicrobial, susceptible cells and persister cells.
2. *Performing processes as mathematical expressions.* In our case, this is the system of four partial di ferential equations describing the evolution of substrate, antimicrobial, susceptible and persister cells.
3. *The mathematical expressions are combined together appropriately in equations.* We will discuss this more clearly in chapter 3.
4. *The parameters involved in the mathematical expressions are given values.* In our model, parameters come from real experiments.
5. Approximation the solution of the system by numerical methods. If the problem has a solution, then we approximate it by a numerical scheme. See more in chapter 4.
6. *The properties of the system are explored via the solution of the model.*

1.4 Why do we use Mathematics for studying biofilms?

Above presence of biofilms in a wide range of situations has led the researchers to study their properties both for their good and bad aspect. It turns out that mathematical modeling can be an efficient and essential tool for the study of biofilms.

Modeling is a powerful tool for studying biofilm processes, as well as for understanding how to encourage good biofilms or discourage bad biofilms. A mathematical model may be a good way to connect the different processes to each other and to measure their relative contributions [13].

In our problem, we will use the finite element method (mentioned in Chapter 2) to approximate the solution of the PDE system. Then, base on numerical results, we will propose a strategy to dosing antimicrobial effectively.

Chapter 2

Finite Element Method

In this chapter, I mainly mention about fundamental knowledge of Finite Element Method (FEM) which I have used in this report. It is not a full statement about FEM.

2.1 Introduction to FEM

The mathematical models of science and technology are mainly in form of differential or integral equations. With the rapid development of computer's strength, using computer-implemented mathematical model, one may have useful tools to simulate or analyse complicated systems in science and engineering. In order to do that, one needs to use the numerical methods. One of popular methods may be mentioned as finite element method which is described as following.

The Finite Element Method (FEM) is a very powerful and flexible numerical approach for solving partial differential equations. Its flexibility means that it can be used to solve complicated equations in domains whose geometries range from a simple polygon or polyhedron such as a square or a cube to more complex shapes with curved boundaries. It is also easy to construct higher-order approximations. However, the programming of finite element methods is more complicated than most other method, and hence in general requires standard software packages. Fortunately, we can use a powerful software called FreeFEM++ which is a finite element solver [1]. We will discuss more about it at appendix A.

In order to approximately solve a given PDE, using FEM, one basically has to go through the following four steps:

1. Write a variational formulation of the problem we consider.
2. Discretize the problem domain using finite elements.
3. Implement the method in a high-level language.
4. Solve the discrete problem.

2.2 Advection-Diffusion-Reaction equation

We first are interested in the advection-diffusion-reaction equation that describes in $\mathbb{R}^2$ which is given by

$$\begin{aligned} -D\Delta u + c \cdot \nabla u + Ru &= f \qquad \text{in } \Omega \subset \mathbb{R}^2, \\ u &= 0 \qquad \text{on } \partial\Omega, \end{aligned} \tag{2.1}$$

with $D > 0$ the diffusion coefficient, $c \in [L^2(\Omega)]^2$ the velocity vector field of flows which are imcompressible (i.e. $\nabla \cdot c = 0$), R the reaction term and $f \in L^2(\Omega)$.

2.2.1 Variational formulation

We obtain the weak form of equation (2.1) by multiplying both sides by a test function $v \in V := H_0^1(\Omega)$, integrating over the domain Ω and performing integration by parts. The result is

$$\int_\Omega D\nabla u \cdot \nabla v + \int_\Omega c \cdot \nabla uv + \int_\Omega Ruv = \int_\Omega fv, \qquad \forall v \in H_0^1(\Omega).$$

If we define, for $u, v \in V$, a real-valued mapping a by

$$a(u, v) := \int_\Omega D\nabla u \cdot \nabla v + \int_\Omega c \cdot \nabla uv + \int_\Omega Ruv, \tag{2.2}$$

and the notion

$$\langle u, v \rangle_0 := \int_\Omega uv \quad \text{for } u, v \in L^2(\Omega),$$

then the problem (2.1) becomes, find $u \in V$ such that

$$a(u, v) = \langle f, v \rangle_0 , \qquad \forall v \in V. \tag{2.3}$$

2.2.2 Existence and Uniqueness

We recall the following the Lax-Milgram theorem ensures the existence and uniqueness of a solution of (2.3) because it is easy to check that a is bilinear, continuous and V-elliptic.

Definition 1. A bilinear form $a : V \times V \to \mathbb{R}$ is said to be

(i) *continuous* if there is a constant M such that

$$|a(u, v)| \leq M|u||v| \qquad \forall u, v \in V, \tag{2.4}$$

(ii) *coercive* (or *V-elliptic*) if there is a constant $\alpha > 0$ such that

$$a(v, v) \geq \alpha \|v\|_V^2 \qquad \forall v \in V. \tag{2.5}$$

Theorem 1. (Lax-Milgram) Given a Hilbert space (V,(.,.)), a bilinear, continuous, coercive form $a \in \mathcal{L}(V \times V; R)$ and a linear functional $f \in V'$, there exists a unique $u \in V$ such that:

$$a(u, v) = f(v), \qquad \forall v \in V.$$

Proof. See the proof of theorem 2.7.7 in [3]. □

2.2.3 Ritz-Galerkin method

To find an approximation to the solution u, by Ritz-Galerkin method, we choose[1] a finite-dimensional subspace V_h of V and ask that equation (2.3) is satisfied only for v in V_h. We will discuss more about triangulation of the domain next section. Then we look for a function $u_h \in V_h$ which satisfies

$$a(u_h, v_h) = \langle f, v_h \rangle_0 \quad \text{for all } v_h \in V_h. \tag{2.6}$$

u_h is called the finite element solution.

Again, by the Lax-Milgram theorem, we know that (2.6) has a unique solution $u_h \in V_h$.

It is easy to see that the Ritz-Galerkin method gives rise to a linear algebraic system, once we specify a basis of V_h. Therefore, let us assume that $\{\phi\}_{j=1}^N$ is a basic of V_h then we can write $u_h = \Sigma_{i=1}^N \alpha_i \phi_i$. By choosing v to be a basic function ϕ_i, then u_h satisfies (2.6) if and only if

$$\sum_{j=1}^{N} a(\phi_j, \phi_i)\alpha_j = \langle f, \phi_i \rangle_0 , \qquad \text{for } i = 1, ..., N.$$

This is really a linear system of the form

$$Ku = F,$$

where $u = (\alpha_1, ..., \alpha_N)$ and

$$K_{ij} = a(\phi_i, \phi_j),$$
$$F_i = \langle f, \phi_i \rangle_0 .$$

K is called the *stiffness matrix* (because the linear system looks like Hooke's law if f represents forces and u represents displacements). Here, K is positive definite (we will not discuss more detail here).

Now, there are two basically major aspects with regard to the construction of appropriate finite-dimensional subspaces V_h

1. Computation efficiency
2. Order of accuracy

In order to reduce computation time, we use finite elements which have local support. Lagrangian finite elements, for example, are a good choice. The order of accuracy is mentioned in the next subsection.

[1] see more about construction of V_h in appendix A.1.3 at page 39

2.2.4 Estimates for general finite element approximation

We now want to estimate the error $\|u - u_h\|_V$ to determine the accuracy of the approximation of the solution u in (2.3) by the solution u_h in (2.6). This estimate is a consequence of following relationships.

Proposition 1. (Fundamental Galerkin Orthogonality) Let u and u_h be solutions to (2.3) and (2.6) respectively. Then

$$a(u - u_h, v) = 0, \qquad \forall v \in V_h.$$

Proof. We have $a(u, v) = \langle f, v \rangle_0, \forall v \in V$ from (2.3) and $a(u_h, v) = \langle f, v \rangle_0, \forall v \in V_h \subset V$ from (2.6). Subtract them, we get the result. □

Theorem 2. (Céa's lemma) Suppose the conditions of Lax-Milgram theorems (cf. Theorem 1) for a hold then

$$\|u - u_h\|_V \leq \frac{M}{\alpha} \min_{v \in V_h} \|u - v\|_V,$$

where M is the continuity constant and α is the coercivity constant of $a(\cdot, \cdot)$ on V.

Proof. See Theorem 2.8.1 of [3]. □

From Theorem 3.29 of [10], if the solution u of (2.1) belongs to $H^{k+1}(\Omega)\,(k \geq 0)$, then for the finite element approximation u_h defined in (2.6), it follows that

$$\|u - u_h\|_1 \leq Ch^2 |u|_2.$$

Moreover, according to Aubin and Nitsche's theorem (cf. Theorem 3.37 of [10]), if $u \in H^{k+1}$ then we also have

$$\|u - u_h\|_0 \leq Ch^{k+1} |u|_{k+1}. \tag{2.7}$$

2.3 Time-dependent problem

Our problem about biofilms is not considered as a steady state,it is a time-dependent problem. In this section, we will discuss about the method to solve this type of the problem.

2.3.1 Problem setting

The domain $\Omega \subset \mathbb{R}^2$ is assumed to be a bounded Lipchitz domain with boundary $\partial\Omega = \Gamma_1 \cup \Gamma_2 \cup \Gamma_3$ where Γ_3 is a closed subset of the boundary. In a space-time cylinder $Q_T = \Omega \times (0,T), T > 0$ and its boundary $S_T = \partial\Omega \times (0,T)$, there are given functions $f : Q_T \to \mathbb{R}, g : S_T \to \mathbb{R}$, $g(x,y;t) = g_i(x,y;t)$ for $(x,y) \in \Gamma_i, i = 1,2,3$ and $u_0 : \Omega \to \mathbb{R}$. The problem is to find a function $u : Q_T \to \mathbb{R}$ such that

$$\begin{aligned} \frac{\partial u}{\partial t} + Lu &= f \quad \text{in} \quad Q_T, \\ Ru &= g \quad \text{on} \quad S_T, \\ u &= u_0 \quad \text{onn} \quad \Omega \times \{0\}, \end{aligned} \tag{2.8}$$

where Lv denotes the differential expression for some function $v : \Omega \to \mathbb{R}$

$$(Lv)(x,y) := -\nabla \cdot (K(x,y)\nabla v(x,y)) + c(x,y) \cdot \nabla v(x,y) + r(x,y)v(x,y),$$

with sufficiently smooth, time-independent coefficients

$$K : \Omega \to \mathbb{R}^{2,2}, \quad c : \Omega \to \mathbb{R}^2, \quad r : \Omega \to \mathbb{R}.$$

The boundary condition is expressed by the shorthand notation $Ru = g$, which means, for a function $\alpha : \Gamma_2 \to \mathbb{R}$ on $\partial\Omega$,

- Neumann boundary condition

  $$\nabla u \cdot \mathbf{n} = g_1 \quad \text{on } \Gamma_1 \times (0,T),$$

  with the outer unit normal $\mathbf{n}$

- Mixed boundary condition

  $$\nabla u \cdot \mathbf{n} + \alpha u = g2 \quad \text{on } \Gamma_2 \times (0,T).$$

- Dirichlet boundary condition

  $$u = g_3 \quad \text{on } \Gamma_3 \times (0,T).$$

Definition 2. (Norm of space $L^p((0,T),X)$) The space $L^p((0,T),X)$ with $1 \le p \le \infty$ consists of all functions on $(0,T) \times \Omega$ with the following properties

$v(t,\cdot) \in X$ for any $t \in (0,T), F \in L^p(0,T)$ with $F(t) := \|v(t,\cdot)\|_X$.

Furthermore,

$$\|v\|_{L^p((0,T),X)} := \|F\|_{L^p(0,T)}.$$

2.3.2 Weak solutions of time-dependent problem

Definition 3. (Weak derivative) A function $u \in L^2((0,T),V)$ is said to have a *weak derivative* w if the following holds

$$\int_0^T u(t)\phi'(t)dt = -\int_0^T w(t)\phi(t)dt \quad \forall \phi \in C_0^\infty(0,T).$$

Usually, this derivative w is denoted by $\frac{du}{dt}$ or u'

Before we give a weak formulation of (2.8), we denote

$$a(u,v) := \int_\Omega [K\nabla u \cdot \nabla v + (c \cdot \nabla u + ru)]dx + \int_{\Gamma_2} \alpha uv d\sigma, u, v \in V.$$

Let $u_0 \in H := L^2(\Omega), f \in L^2((0,T),H)$ and in case of Dirichlet we restrict our case to the homogeneous case.

Definition 4. (Weak solution) An element $u \in L^2((0,T),V)$ is called a *weak derivative* of (2.8) if it has a weak derivative $u' \in L^2((0,T),H)$ and the following holds

$$\begin{aligned} \langle u_t(t), v\rangle_0 + a(u(t),v) = \langle f(t), v\rangle_0 &+ \int_{\Gamma_1} g_1(\cdot,t)v d\sigma \\ &+ \int_{\Gamma_2} g_2(\cdot,t)v d\sigma \\ &\text{for all } v \in V, t \in (0,T), \\ u = u_0. & \end{aligned} \tag{2.9}$$

2.3.3 Existence and uniqueness of solution

Theorem 3. (J.L.Lions) Let $V \subset L$ be two Hilbert spaces with continuous embedding and

$$\forall v \in V, c_P \|v\|_L^2 \leq \|v\|_V^2 .$$

Consider the mapping $a :]0,T[\times V \times V \to \mathbb{R}$ such that $a(t,\cdot,\cdot)$ is bilinear for a.e. in $]0,T[$ and for all $u \in V$.

If a satisfies the following properties:

(i) The function $t \to a(t,u,v)$ is measurable $\forall u, v \in V$.

(ii) $\exists M$ such that $|a(t,u,v) \leq M \|u\|_V |v|_V$ for a.e. $t \in [0,T], \forall u, v \in V$.

(iii) $\exists \alpha > 0$ and $\gamma > 0$ such that $a(t,u,u) \geq \alpha \|u\|_V^2 - \gamma \|u\|_L^2$ for a.e. $t \in [0,T]$ and for all $u \in V$.

For $f \in L^2(]0,T[;V')$ and $u_0 \in L$, the following problem has unique solution:

$$\begin{cases} \text{Seek } u \in W(v,v') \text{ such that} \\ \langle d_t u, v\rangle_{V,V'} + a(t,u,v) = \langle f(t), v\rangle_{V,V'} \text{, a.e. } t \in]0,T[, \forall v \in V, \\ u(0) = u_0 \end{cases}$$

Proof. See the proof of theorem 6.6 in [9]. □

2.3.4 Fully discrete scheme

For solving our problem numerically, a wide variety of methods exists. Here we only consider one of them, which consists in using an Euler scheme in time and a finite element scheme in space. . More particularly, we will use one-step discretizations for finite element method (cf. [10]).

We proceed to apply the finite element method to (2.9) for every fixed $t \in (0,T)$, using the abbreviation

$$b(t,v) := \langle f(t), v\rangle_0 + \int_{\Gamma_1} g_1(\cdot,t) v d\sigma + \int_{\Gamma_2} g_2(\cdot,t) v d\sigma. \tag{2.10}$$

So let $V_h \subset V$ denote a finite-dimensional subspace and let $u_{0h} \in V_h$ be some approximation to u_0. Then the *semidiscrete-problem* reads follows

Find $u_h \in L^2((0,T),V_h)$ with $u' \in L^2((0,T),H), u_h(0) = u_{0h}$ and

$$\left\langle \frac{d}{dt} u_h(t), v_h \right\rangle_0 + a(u_h(t), v_h) = b(t, v_h) \quad \text{for all } v_h \in V_h, t \in (0,T). \tag{2.11}$$

Let $0 = t_0 < t_1 < ... < t_N = T$ be a discretization of $[0,T]$ and $\tau_n = t_{n+1} - t_n$, we use the approximations

$$\frac{\partial u}{\partial t}(x,y,t) \simeq \frac{u_h^{n+1} - u_h^n}{\tau_n} \qquad \text{with } u_h^n \simeq u_h(t_n).$$

Let[2] U^n be an approximation of $u_h \in V_h$ at time $t = t_n$. The one-step discretization approach can applied directly to (2.11). With $\partial U^{n+1} := (U^{n+1} - U^n/\tau_n)$, $f^{n+s} := sf(t_{n+1}) + (1-s)f(t_n)$, $n^{n+s}(v) := sb(t_{n+1},v) + (1-s)b(t_n,v)$, b according to (2.10), $s \in [0,1]$, and with a fixed number $\Theta \in [0,1], \overline{\Theta} = 1 - \Theta$, the fully discrete method for (2.11) then reads as follows.

Find a sequence $U^0, ..., U^N \in V_h$ such that for $n \in \{0, ..., N-1\}$,

$$\begin{aligned} \left\langle \partial U^{n+1}, v_h \right\rangle_0 + a(\Theta U^{n+1} + \overline{\Theta} U^n, v_h) &= b^{n+\Theta}(v_h) \\ &\text{for all } v_h \in V_h \\ U^0 &= u_{0h}. \end{aligned} \tag{2.12}$$

[2]The finite element method allows us to consider directly a function U from the finite-dimensional approximation space V_h and thus from the underline function space V [10].

2.3.5 Order of convergence estimates

Definition 5. (Ritz projection) For a V-elliptic, continuous bilinear form $a : V \times V \to \mathbb{R}$, the Ritz, or elliptic, projection $R_h : V \to V_h$ is defined by

$$v \mapsto R_h v \Leftrightarrow a(R_h v - v, v_h) = 0 \qquad \forall v_h \in V_h.$$

Theorem 4. Under the assumption of Definition 5, we have

(i) $R_h : V \to V_h$ is linear continuous.

(ii) R_h yields quasi-optimal approximations, that is,

$$\|v - R_h v\|_V \leq \frac{M}{\alpha} \inf_{u_h \in V_h} \|u - u_h\|_0,$$

where M and α are the Lipschitz and ellipticity constants according to (2.4) and (2.5).

Proof. See the proof of Theorem 7.9 in [10]. □

Moreover, if the bilinear form a defines an elliptic problem such that for the elliptic projection an error estimate of the type

$$\|(I - R_h)w\|_0 \leq Ch^2 \|w\|_0 \qquad \text{for all } w \in V \cap H^2(\Omega), \tag{2.13}$$

is valid (cf. [10]).

Theorem 5. Let a be a V-elliptic, continuous bilinear form, $u_{0h} \in V_h, u_0 \in V, \Theta \in [\frac{1}{2}, 1]$. If $u \in C^2([0,T], V)$, then

$$\begin{aligned}\|u(t_n) - U^n\|_0 \leq \|u_{0h} - R_h u_0\|_0 + \|(I - R_h)u(t_n)\|_0 \\ + \int_0^{t_n} \|(I - R_h)u'(s)\|_0 ds + \tau_n \int_0^{t_n} \|u''(s)\|_0 ds.\end{aligned}$$

Proof. See the proof of Theorem 7.31 in [10]. □

With assumption $u_0 \in V \cap H^2(\Omega)$, applying (2.13) and (2.7), we get

$$\begin{aligned}\|u_{0h} - R_h u_0\|_0 \leq \|u_{0h} - u_0\|_0 + \|u_0 - R_h u_0\|_0 \leq C_1 h^2 \|u_0\|_0, \\ \|(I - R_h)u(t_n)\|_0 = \|u(t_n) - R_h u(t_n)\|_0 \leq C_2 h^2 \|u(t_n)\|_2, \\ \int_0^{t_n} \|(I - R_h)u'(s)\|_0 ds \leq C_3 h^2 \int_0^{t_n} \|u'(s)\|_2 ds,\end{aligned}$$

with C_1, C_2, C_3 are positive constants depending only on u.

These imply

$$\|u(t_n) - U^n\|_0 \leq C(u)(h^2 + \tau_n),$$

with $C(u) > 0$ depending on the solution u (and thus on u_0) but not depending on h and τ_n.

Proposition 2. Let u be the solution of (2.8) and u_h be the solution of (2.11), we have the following convergence result

$$u_h(t_n) \xrightarrow[\tau_n \to 0]{h \to 0} u(t_n),$$

or we will get (with $\tau_n \mapsto 0$) $u_h \mapsto u$.

Proof. Deduce directly from the results of Theorem 5. □

Chapter 3

Mathematical modeling of the resistance of biofilms in antimicrobial

3.1 Overview

In our main investigation, we describe a mathematical model of the dynamics of the susceptible and persister bacterial cells with one growth limiting substrate under presence of a single antimicrobial agent and a neutralizing agent which reacts to the antimicrobial. Most of assumptions and parameters will be learned from documents of N. Cogan [4, 5, 6] and Stewart [12].

We will work on the domain which contains only two regions, the fluid flows and the biofilm region. These two regions is separated by the biofilm interface which is thin enough not to be considered. We also treat the problem in two dimensions that takes into account the fact that some bacteria cells which are not susceptible to the antimicrobial revert back to susceptible cells rather than other ones.

Our model includes the coupled motion of the biofilm and the bulk fluid as well as diffusion/advection of various constituents. To determine the various model components for each time-step, we determine the fluid and biofilm velocities as described below. The diffusion and velocity are also different between external fluid and the internal biofilm.

Finally, the bacteria concentration (susceptible or persister cells) are determined by solving a system of conservation equations that includes mutual effect between bacteria with nutrient and antimicrobial agent.

3.2 Computational domain

We consider a physical domain Ω consisting of a channel of width mL and length L $(m, L > 0)$ and the boundary $\partial\Omega = \Gamma_1 \cup \Gamma_2 \cup \Gamma_3 \cup \Gamma_4 \cup \Gamma_5 \cup \Gamma_6$ as in figure 3.1. In the channel we assume that there is a steady, creeping flow and that there is a biofilm attached to the bottom of the

domain. The biofilm region is bounded by a fluid/biofilm interface, denoted as Γ_7 (see figure 3.1). In the numerical test, for simplicity, we will use the biofilm interface like a top half of the ellipse.

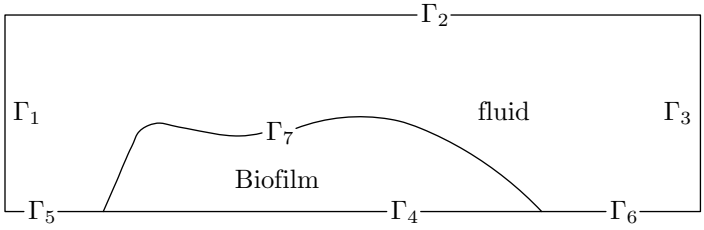

Figure 3.1: A schematic description of the biofilm in Ω and the boundary $\partial\Omega$

3.3 Mathematical model

We denote the bacterial phenotype as B_s and B_p for susceptible and persister density, respectively. We also denote the concentration of nutrient and antimicrobial agent as S and A, respectively. These quantities will depend on both the space and time. The evolution of these constituents is described by a time-dependent advection-diffusion-reaction equation.

3.3.1 Constituents

The nutrient , $S(x, y; t)$, and the antimicrobial agent, $A(x, y; t)$, are introduced into the domain at the left end of the domain. Both are advected by the fluid and diffuse in the whole domain.

The diffusion coefficients of the nutrient and antimicrobial agent, D_s and D_a, are assumed to be smaller in the biofilm region than in the flow region. The reduction factors are denoted as r_s and r_a, respectively. Here, we assume that the coefficients in biofilm region is only 90% compared with the ones outside.

Both nutrient and antimicrobial are fed into the domain at the upstream end of channel, so the Dirichlet boundary conditions are applied at $x = 0$. Standard outflow conditions are applied at the effluent end of the channel. The wall of the channel are not permeable to the constituents, so we apply no-flux boundary conditions here.

We also assume that the nutrient concentration is consumed only by the susceptible population. This consumption is modeled by Monod kinetics, where μ_s, Y_s and K_s denote the maximum specific growth rate, yield coefficient and Monod coefficient, respectively. Therefore, the equation governing the nutrient concentration is,

$$\frac{\partial S}{\partial t} + u \cdot \nabla S - \nabla \cdot (D_s \nabla S) + \mu_S \frac{S}{K_s + S} B_s = 0, \tag{3.1}$$

with boundary conditions

$$\begin{aligned} S(0,y;t) &= S_1 \text{ on } \Gamma_1 \text{ (Dirichlet BC)},\\ (\nabla S \cdot \mathbf{n})(x,y;t) &= 0 \text{ on } \Gamma_2 \cup \Gamma_4 \cup \Gamma_5 \cup \Gamma_6 \text{ (no-flux BC)}, \end{aligned} \tag{3.2}$$

and the initial condition ($S_0 is a given value$)

$$S(x,y;t) = S_0, \tag{3.3}$$

while the antimicrobial agent is governed by

$$\frac{\partial A}{\partial t} + u \cdot \nabla A - \nabla \cdot (D_a \nabla A) + H_a(A,N) = 0, \tag{3.4}$$

where the function H_a describes the reaction between the antimicrobial agent and the concentration of neutralizing agent, denoted as N. For simulation, we assume that H_a is either zero or, if not, we set $H_a = k_r AN$ where k_r is the neutrializer reaction rate coefficient (cf. [6]).

The boundary condition for antimicrobial agent is

$$\begin{aligned} A(0,y;t) &= A_1 \text{ on } \Gamma_1 \text{ (Dirichlet BC)},\\ (\nabla A \cdot \mathbf{n})(x,y;t) &= 0 \text{ on } \Gamma_2 \cup \Gamma_4 \cup \Gamma_5 \cup \Gamma_6 \text{ (no-flux BC)}, \end{aligned} \tag{3.5}$$

while the initial condition ($A_0 is a given value$) is

$$A(x,y;t) = A_0. \tag{3.6}$$

3.3.2 Bacteria

Firstly, we will construct the model of susceptible cells, $B_s(x,y;t)$. Their population *change* due to growth, *death* due to antibiotic (antimicrobial) action, *loss* due to transition to persiter cells and *gain* from reversion of the persister cells (cf. [4]). Therefore, in general, the dynamics of susceptible cells is given in the form of,

$$\frac{dB_s}{dt} = \underbrace{g(B_s,S)}_{\text{Growth}} - \underbrace{d(B_s,S,A)}_{\text{Disinfection}} - \underbrace{l(B_s,S,A)}_{\text{Loss}} + \underbrace{r(B_p,S,A)}_{\text{Reversion}}. \tag{3.7}$$

According to Cogan [4], the growth term is describe by Monod kinetics mentioned in the nutrient construction before. This term is given by

$$g(B_s,S) = \frac{\mu_{max}}{Y}\frac{S}{K_s+S}B_s. \tag{3.8}$$

Disinfection depends on the antimicrobial agent (type of antibiotic). We model this term as follows. Here the function $k_d(A,t)$ depends on the antibiotic concentration. In particular, $k_d = 0$ if $A = 0$ and is nonzero otherwise. Since the problem is time-dependent, the disinfection rates also depend on time.

$$d(Bs,S,A) = k_d(A,t)\mu_{max}\frac{S+\alpha}{K_s+S}B_s. \tag{3.9}$$

We assume that the loss of susceptible cells due to transition to persister occurs at a rate depends on both the growth rate and the antibiotic. Mathematically, we have the following form. In this form, k_l is also time dependent.

$$l(B_s, S, A) = k_l(A, t)\mu_{max}\frac{S}{K_s + S}B_s. \tag{3.10}$$

The last terms, we assume that persister cells only revert to susceptible cells if there is no applied antibiotic and otherwise. So we apply $k_g = 0$ if A is nonzero and otherwise. Then we have the form of reversion term,

$$r(B_p, S, A) = k_g(A, t)B_p.$$

Combine all of these terms with (3.7) we have the mathematical model of susceptible cells

$$\frac{\partial B_s}{\partial t} + u \cdot \nabla B_s - \hat{k_s}(S)B_s + \hat{k_d}(S)B_s + \hat{k_l}(S)B_s - \hat{k_g}B_p = 0, \tag{3.11}$$

where,

- $\hat{k}_s(S) = \dfrac{\mu_{max}}{Y}\dfrac{S}{K_S + S}$,
- $\hat{k}_d(S) = k_d(A, t)\dfrac{\mu_{max}}{Y}\dfrac{S}{K_s + S}$,
- $\hat{k}_l(S) = k_l(A, t)\dfrac{\mu_{max}}{Y}\dfrac{S}{K_S + S}$,
- $\hat{k}_g = k_g(A, t)$.

Persister cells gain from transition of susceptible cells and only change when they convert to susceptible cells. Therefore, the dynamics of persister cells are

$$\frac{\partial B_p}{\partial t} + u \cdot \nabla B_p - \hat{k}_l(S)B_s + k_g(A, t)B_p = 0. \tag{3.12}$$

In [5], bacteria is assumed to be zero outside the biofilm region. We also impose no-flux boundary condition on the channel walls and Dirichlet conditions at the influent end. At the effluent end, we impose outflow conditions allowing the bacteria to be transported out of the domain. From all of these assumptions, we have the boundary conditions of susceptible cells and persister cells,

$$\begin{aligned}
&B_s(x, y; t) = 0 \text{ on } \Gamma_1 \cup \Gamma_2 \cup \Gamma_3 \cup \Gamma_5 \cup \Gamma_6,\\
&B_s(x, y; t) = B_s^1 \text{ on } \Gamma_4,\\
&B_p(x, y; t) = 0 \text{ on } \Gamma_1 \cup \Gamma_2 \cup \Gamma_3 \cup \Gamma_5 \cup \Gamma_6,\\
&B_p(x, y; t) = B_p^1 \text{ on } \Gamma_4,
\end{aligned} \tag{3.13}$$

and the initial conditions (B_s^0, B_p^0 are given values)

$$\begin{aligned}
B_s(x, y; 0) &= B_s^0,\\
B_p(x, y; 0) &= B_p^0.
\end{aligned} \tag{3.14}$$

Summarize from (3.1), (3.4), (3.7), (3.12), we need to find (S, A, B_s, B_p) such that the following system

$$\begin{cases} \partial_t S + u \cdot \nabla S - \nabla \cdot (D_s \nabla S) + \mu_S \dfrac{S}{K_s + S} B_s = 0, \\ \partial_t A + u \cdot \nabla A - \nabla \cdot (D_a \nabla A) + k_r N A = 0, \\ \partial_t B_s + u \cdot \nabla B_s - \hat{k_s}(S) B_s + \hat{k_d}(S) B_s + \hat{k_l}(S) B_s - \hat{k_g}(A,t) B_p = 0, \\ \partial_t B_p + u \cdot \nabla B_p - \hat{k_l}(S) B_s + \hat{k_g}(A,t) B_p = 0. \end{cases} \tag{3.15}$$

with boundary conditions summarized from (3.2),(3.5), (3.13):

$$\begin{aligned} S(x,y;t) &= S_1 \text{ on } \Gamma_1, \\ (\nabla S \cdot \mathbf{n})(x,y;t) &= 0 \text{ on } \Gamma_2 \cup \Gamma_4 \cup \Gamma_5 \cup \Gamma_6, \\ A(x,y;t) &= A_1 \text{ on } \Gamma_1, \\ (\nabla A \cdot \mathbf{n})(x,y;t) &= 0 \text{ on } \Gamma_2 \cup \Gamma_4 \cup \Gamma_5 \cup \Gamma_6, \\ B_s(x,y,t) &= 0 \text{ on } \Gamma_1 \cup \Gamma_2 \cup \Gamma_3 \cup \Gamma_5 \cup \Gamma_6. \\ B_s(x,y,t) &= B_s^1 \text{ on } \Gamma_4. \\ B_p(x,y,t) &= 0 \text{ on } \Gamma_1 \cup \Gamma_2 \cup \Gamma_3 \cup \Gamma_5 \cup \Gamma_6. \\ B_p(x,y,t) &= B_p^1 \text{ on } \Gamma_4. \end{aligned} \tag{3.16}$$

and initial conditions summarized from (3.3), (3.6), (3.14) on Ω:

$$\begin{aligned} S(x,y,0) &= S_0. \\ A(x,y,0) &= A_0. \\ B_s(x,y,0) &= B_s^0. \\ B_p(x,y,0) &= B_p^0. \end{aligned} \tag{3.17}$$

3.4 Variational formulation

Let $V_1 = \{w \in H^1(\Omega) | w = 0 \text{ on } \Gamma_1 \cup \Gamma_3\}$, $V_2 = \{w \in H^1(\Omega) | w = 0 \text{ on } \Gamma_1 \cup \Gamma_2 \cup \Gamma_3 \cup \Gamma_5 \cup \Gamma_6\}$ and $V = L^2(V_1) \times L^2(V_1) \times L^2(V_2) \times L^2(V_2)$. A weak formulation of (3.15), (3.16), (3.17) consists in finding $(S, A, B_s, B_p) \in V$ such that

$$\begin{cases} \displaystyle\int_\Omega \partial_t S v + \int_\Omega u \cdot \nabla S v + \int_\Omega D_s \nabla S \cdot \nabla v + \mu_s \int_\Omega \frac{S}{K_s + S} B_s v = 0, \quad \forall v \in V_1. \\ \displaystyle\int_\Omega \partial_t A v + \int_\Omega u \cdot \nabla A v + \int_\Omega D_a \nabla A \cdot \nabla v + \int_\Omega k_r N A v = 0, \quad \forall v \in V_1. \\ \displaystyle\int_\Omega \partial_t B_s v + \int_\Omega u \cdot \nabla B_s v - \int_\Omega \hat{k_s}(S) B_s v + \int_\Omega \hat{k_d}(S) B_s v + \int_\Omega \hat{k_l}(S) B_s v \\ \qquad\qquad - \int_\Omega \hat{k_g} B_p v = 0, \ \forall v \in V_2. \\ \displaystyle\int_\Omega \partial_t B_p v + \int_\Omega u \cdot \nabla B_p v - \int_\Omega \hat{k_l}(S) B_s v + \int_\Omega \hat{k_g} B_p v = 0, \quad \forall v \in V_2. \end{cases} \tag{3.18}$$

3.5 Finite element discretization

Let $\{\mathcal{T}_h\}_h$ be a regular family of triangulation (cf. Definition 7) of Ω in sense that for each h:

- $\overline{\Omega}$ is the union of all elements of $\mathcal{T}_h$;
- The intersection of two different elements of $\mathcal{T}_h$, if not empty, is a vertex or a whole edge;
- The ratio of the diameter h_K of any element K of $\mathcal{T}_h$ to the diameter of its inscribed circle is smaller than a constant independent of h where h stands for the maximum of the diameters h_K, $K \in \mathcal{T}_h$;

We consider the finite element space V_h such that

$$V_h = \{v_h \in H^1(\Omega) : v_h|_T \in \mathbb{P}^1(T), \forall T \in \mathcal{T}_h\},$$

where $\mathbb{P}^1(T)$ is the space of polynomials of degree at most 1.

Let $W_h^1 = V_h \cap V_1 = \{v_h \in H^1(\Omega) | v_h = 0 \text{ on } \Gamma_1 \cup \Gamma_3, v_h|_T \in \mathbb{P}^1(T), \forall T \in \mathcal{T}_h\}$, $W_h^2 = V_h \cap V_2 = \{v_h \in H^1(\Omega) | v_h = 0 \text{ on } \Gamma_1 \cup \Gamma_2 \cup \Gamma_3 \cup \Gamma_5 \cup \Gamma_6, v_h|_T \in \mathbb{P}^1(T), \forall T \in \mathcal{T}_h\}$ then the problem reads as follows:

Find $(S_h, A_h, B_{sh}, B_{ph}) \in L^2(W_h^1) \times L^2(W_h^1) \times L^2(W_h^2) \times L^2(W_h^2)$ such that:

$$\begin{cases} \displaystyle\int_\Omega \partial_t S_h v_h + \int_\Omega u \cdot \nabla S_h v_h + \int_\Omega D_s \nabla S_h \cdot \nabla v_h \\ \qquad\qquad + \mu_s \displaystyle\int_\Omega \frac{S_h}{K_s + S_h} B_{s,h} v_h = 0, \quad \forall v_h \in W_h^1, \\ \displaystyle\int_\Omega \partial_t S_h v_h + \int_\Omega u \cdot \nabla A_h v_h + \int_\Omega D_a \nabla A_h \cdot \nabla v_h + \int_\Omega k_r N A_h v_h = 0, \quad \forall v_h \in W_h^1, \\ \displaystyle\int_\Omega \partial_t B_{sh} v_h + \int_\Omega u \cdot \nabla B_{sh} v_h - \int_\Omega \hat{k_s}(S_h) B_{sh} v_h + \int_\Omega \hat{k_d}(S_h) B_{sh} v_h + \\ \qquad\qquad + \displaystyle\int_\Omega \hat{k_l}(S_h) B_{sh} v_h - \int_\Omega \hat{k_g} B_{ph} v_h = 0, \quad \forall v_h \in W_h^2, \\ \displaystyle\int_\Omega \partial_t B_{ph} v_h + \int_\Omega u \cdot \nabla B_{ph} v_h - \int_\Omega \hat{k_l}(S_h) B_{sh} v_h + \int_\Omega \hat{k_g} B_{ph} v_h = 0, \quad \forall v_h \in W_h^2. \end{cases} \tag{3.19}$$

3.6 Time discretization

Let $0 = t_0 < t_1 < ... < t_n = T > 0$ be a discretization of $[0, T]$ and $\tau_n = t_{n+1} - t_n$, we will use the approximations:

$$\begin{aligned}
\frac{\partial S_h}{\partial t}(x, y, t_n) &\simeq \frac{S_h^{n+1} - S_h^n}{\tau_n} \quad \text{with } S_h^n \simeq S_h(t_n).\\
\frac{\partial A_h}{\partial t}(x, y, t_n) &\simeq \frac{A_h^{n+1} - A_h^n}{\tau_n} \quad \text{with } A_h^n \simeq A_h(t_n).\\
\frac{\partial B_{sh}}{\partial t}(x, y, t_n) &\simeq \frac{B_{sh}^{n+1} - B_{sh}^n}{\tau_n} \quad \text{with } B_{sh}^n \simeq B_{sh}(t_n).\\
\frac{\partial B_{ph}}{\partial t}(x, y, t_n) &\simeq \frac{B_{ph}^{n+1} - B_{ph}^n}{\tau_n} \quad \text{with } B_{ph}^n \simeq B_{ph}(t_n).
\end{aligned}$$

Let us denote $\mathbf{S}^n, \mathbf{A}^n, \mathbf{B}_s^n, \mathbf{B}_p^n$ by $S_h(t^n), A_h(t^n), B_{sh}(t_n), B_{ph}(t^n)$ respectively.

For convenient, we introduce some useful notations:

$$\begin{aligned}
X_1 = S, X_2 = A, X_3 = B_s, X_4 = B_p.\\
\mathbf{X}_1^n = \mathbf{S}^n, \mathbf{X}_1^n = \mathbf{A}^n, \mathbf{X}_3^n = \mathbf{B}_s^n, \mathbf{X}_4^n = \mathbf{B}_p^n.\\
\alpha_1 = D_s, \alpha_2 = D_a, \alpha_3 = \alpha_4 = 0.\\
f(\mathbf{X}_1^n) = f(\mathbf{S}^n) = \frac{\mathbf{B}_s^n}{K_s + \mathbf{S}^n}.\\
f(\mathbf{X}_2^n) = f(\mathbf{A}^n) = -k_r N.\\
f(\mathbf{X}_3^n) = f(\mathbf{B}_s^n) = \hat{k_s}(\mathbf{S}^n) + \hat{k}_d(\mathbf{S}^n) + \hat{k}_l(\mathbf{S}^n).\\
f(\mathbf{X}_4^n) = f(\mathbf{B}_p^n) = \hat{k}_g.\\
g(X_1) = g(X_2) = 0.\\
g(X_3) = \int_\Omega \hat{k}_g B_p v_h.\\
g(X_4) = \int_\Omega \hat{k}_l B_s v_h.
\end{aligned} \tag{3.20}$$

the notations of spaces are

$$\begin{aligned}
Q_1 = Q_2 = V_1.\\
Q_3 = Q_4 = V_2.\\
G_1 = G_2 = W_h^1.\\
G_3 = G_4 = W_h^2.
\end{aligned}$$

and an operator a is defined at the time $t = t_n$

$$a(\mathbf{X}_i^{n+1}, v) = \int_\Omega \alpha_i \nabla \mathbf{X}_i^{n+1} \cdot \nabla v + \int_\Omega u \cdot \nabla \mathbf{X}_i^{n+1} v + \int_\Omega f(\mathbf{X}_i^n) \mathbf{X}_i^{n+1} v, \quad \forall v \in G_i, \text{ for } i \in \overline{1,4}.$$

With[1] $\Theta \in [0,1], \overline{\Theta} = 1 - \Theta$, the fully discrete method for (3.19) then reads as follows:

Find a sequence $\mathbf{X}_i^0, \mathbf{X}_i^1, ..., \mathbf{X}_i^N$ in $L^2(G_i)$ such that for $n \in \{0, 1, ..., N-1\}$,

$$\left\langle \partial \mathbf{X}_i^{n+1}, v_h \right\rangle_0 + a(\Theta \mathbf{X}_i^{n+1} + \overline{\Theta} \mathbf{X}_i^n, v_h) = g(\mathbf{X}_i^n), \qquad \forall v_h \in G_i, \text{ for } i \in \overline{1,4}. \tag{3.21}$$

3.7 Existence and Uniqueness

With assumptions $\|u\|_\infty < +\infty$ and $\mathbf{n} \cdot u > 0$, we now prove that the problem (3.21) with boundary conditions (3.16) and initial conditions (3.17) has a unique solution by using Lax-Milgram theorem (cf. Theorem 1) and Lions theorem (cf. Theorem 3). Indeed,for $i \in \overline{1,4}$ we have:

- a is bilinear:

$$\begin{aligned}
a(\mathbf{X}_{i1}^{n+1} + \beta \mathbf{X}_{i2}^{n+1}, v_h) &= \int_\Omega u \cdot \nabla(\mathbf{X}_{i1}^{n+1} + \beta \mathbf{X}_{i2}^{n+1}) v_h + \alpha \int_\Omega \nabla(\mathbf{X}_{i1}^{n+1} + \beta \mathbf{X}_{i2}^{n+1}) \cdot \nabla v_h \\
&\quad + \int_\Omega f(\mathbf{X}_i^n)(\mathbf{X}_{i1}^{n+1} + \beta \mathbf{X}_{i2}^{n+1}) v_h \\
&= \int_\Omega u \cdot \nabla \mathbf{X}_{i1}^{n+1} v_h + \alpha \int_\Omega \nabla \mathbf{X}_{i1}^{n+1} \cdot \nabla v_h + \int_\Omega f(\mathbf{X}_i^n) \mathbf{X}_{i1}^{n+1} v_h \\
&\quad + \beta \left(\int_\Omega u \cdot \nabla \mathbf{X}_{i2}^{n+1} v_h + \alpha \int_\Omega \nabla \mathbf{X}_{i2}^{n+1} \cdot \nabla v_h + \int_\Omega f(\mathbf{X}_i^n) \mathbf{X}_{i2}^{n+1} v_h \right) \\
&= a(\mathbf{X}_{i1}^{n+1}, v_h) + \beta a(\mathbf{X}_{i2}^{n+1}, v_h).
\end{aligned}$$

$$\begin{aligned}
a(\mathbf{X}_i^{n+1}, v_{1h} + \beta v_{2h}) &= \int_\Omega u \cdot \nabla \mathbf{X}_i^{n+1} (v_{1h} + \beta v_{2h}) + \alpha \int_\Omega \nabla \mathbf{X}_i^{n+1} \cdot \nabla (v_{1h} + \beta v_{2h}) \\
&\quad + \int_\Omega f(\mathbf{X}_i^n) \mathbf{X}_i^{n+1} (v_{1h} + \beta v_{2h}) \\
&= \int_\Omega u \cdot \nabla \mathbf{X}_i^{n+1} v_{1h} + \alpha \int_\Omega \nabla \mathbf{X}_i^{n+1} \cdot \nabla v_{1h} + \int_\Omega f(\mathbf{X}_i^n) \mathbf{X}_i^{n+1} v_{1h} \\
&\quad + \beta \left(\int_\Omega u \cdot \nabla \mathbf{X}_i^{n+1} v_{2h} + \alpha \int_\Omega \nabla \mathbf{X}_i^{n+1} \cdot \nabla v_{2h} + \int_\Omega f(\mathbf{X}_i^n) \mathbf{X}_i^{n+1} v_{2h} \right) \\
&= a(\mathbf{X}_i^{n+1}, v_{1h}) + \beta a(\mathbf{X}_i^{n+1}, v_{2h}).
\end{aligned}$$

- The function $t \mapsto a(t, X_i, v)$ is measurable. That is reasonable because X_i is in $L^2(Q_i)$. In other words,

$$\int_0^T |a(t, X_i, v)| \leq \int_0^T \left| \int_\Omega \alpha \nabla X_i \cdot v \right| + \int_0^T \left| \int_\Omega u \cdot \nabla X_i v \right| + \int_0^T \left| \int_\Omega f(X_i) X_i v \right| < +\infty.$$

[1] $\Theta = 0$ for explicit scheme and $\Theta = 1$ for implicit one.

- a is continuous:

$$\begin{aligned}\left|a(\mathbf{X}_i^{n+1}, v_h)\right| &\leq \left|\int_\Omega u\cdot\nabla\mathbf{X}_i^{n+1}v_h\right| + \alpha\left|\int_\Omega \nabla\mathbf{X}_i^{n+1}\cdot\nabla v_h\right| + \left|\int_\Omega f(\mathbf{X}_i^n)\mathbf{X}_i^{n+1}v_h\right| \\ &\leq \int_\Omega |u||\nabla\mathbf{X}_i^{n+1}||v_h| + C_1\left\|\nabla\mathbf{X}_i^{n+1}\right\|_2\|\nabla v_h\|_2 + C_2\left\|\mathbf{X}_i^{n+1}\right\|_2\|v_h\|_2 \\ &\leq C_3\left\|\nabla\mathbf{X}_i^{n+1}\right\|_2\|v_h\|_2 + C_1\left\|\nabla\mathbf{X}_i^{n+1}\right\|_2\|\nabla v_h\|_2 + C_2\left\|\mathbf{X}_i^{n+1}\right\|_2\|v_h\|_2 \\ &\leq M\left(\left\|\mathbf{X}_i^{n+1}\right\|_{G_i}\|v_h\|_{G_i}\right) \quad .\end{aligned}$$

  where C_1, C_2, C_3, M are positive constants and $|\cdot|$ denotes the absolute value of a real number or the Euclidean norm of a vector. Here we have used the Holder inequality at the second inequality.

- a is V-elliptic:

$$\begin{aligned}a(\mathbf{X}_i^{n+1}, \mathbf{X}_i^{n+1}) &= \int_\Omega (u\cdot\nabla\mathbf{X}^{n+1})\mathbf{X}_i^{n+1} + \alpha\int_\Omega\left|\nabla\mathbf{X}_i^{n+1}\right|^2 + \int_\Omega f(\mathbf{X}_i^n)\left|\mathbf{S}^{n+1}\right|^2 \\ &\geq \frac{1}{2}\int_\Omega u\cdot\nabla(\mathbf{X}_i{}^{n+1})^2 + \beta\left(\int_\Omega\left|\nabla\mathbf{X}_i{}^{n+1}\right|^2 + \int_\Omega\left|\mathbf{X}_i{}^{n+1}\right|^2\right) \\ &= -\frac{1}{2}\int_\Omega\underbrace{(\nabla\cdot u)}_{=0}(\mathbf{X}_i^{n+1})^2 + \frac{1}{2}\int_{\partial\Omega}(\mathbf{n}\cdot u)(\mathbf{X}_i^{n+1})^2 + \beta\left\|\mathbf{X}_i^{n+1}\right\|_{G_i} \\ &\geq \beta\left\|\mathbf{X}_i^{n+1}\right\|_{G_i}.\end{aligned}$$

  where $\beta = \inf\{\alpha, f(\mathbf{X}_i^n)\}$

3.8 Convergence of the solution

We will consider only in case $\Theta \in [\frac{1}{2}; 1]$ and then apply the Proposition 2 for (S, A, B_s, B_p) is the solution of (3.18) and $(S_h, A_h, B_{sh}, B_{ph})$ is the solution of (3.19). Then we have

$$(S_h, A_h, B_{sh}, B_{ph}) \mapsto (S, A, B_s, B_p).$$

Therefore, the problem (3.18) has at least one solution. In next section, we will prove that this is the unique solution.

3.9 Uniqueness of the exact solutions

For $i \in \overline{1,4}$, suppose that X_{i1}, X_{i2} are two arbitrary solutions of our main problem satisfying the weak formulation (3.18) for all $v \in Q_i$ then we have

$$\begin{aligned}\langle\partial_t X_{i1}, v\rangle_0 + a(X_{i1}, v) &= g(X_{i1}) \quad \forall v \in Q_i, \\ \langle\partial_t X_{i2}, v\rangle_0 + a(X_{i2}, v) &= g(X_{i2}) \quad \forall v \in Q_i,\end{aligned}$$

Then,

$$\langle \partial_t(X_{i1} - X_{i2}), v\rangle_0 + \langle \alpha\nabla(X_{i1} - X_{i2}), \nabla v\rangle_0 + \langle u \cdot \nabla(X_{i1} - X_{i2}), v\rangle_0 + \langle f(X_{i1})X_{i1}, v\rangle_0 - \langle f(X_{i2})X_{i2}, v\rangle_0 = 0 \quad \forall v \in Q_i.$$

Choose[2] $v = X_{i1} - X_{i2} \in Q_i$, we get:

$$\begin{aligned}\langle \partial_t(X_{i1} - X_{i2}), X_{i1} - X_{i2}\rangle_0 + \langle \alpha\nabla(X_{i1} - X_{i2}), \nabla(X_{i1} - X_{i2})\rangle_0 \\ + \langle u \cdot \nabla(X_{i1} - X_{i2}), X_{i1} - X_{i2}\rangle_0 + \langle f(X_{i1})X_{i1}, X_{i1} - X_{i2}\rangle_0 \\ - \langle f(X_{i2})X_{i2}, X_{i1} - X_{i2}\rangle_0 = 0.\end{aligned} \tag{3.22}$$

Let's consider each term of (3.22). For the first term,using the Leibniz's integral rule, we have:

$$\begin{aligned}\langle \partial_t(X_1 - X_{i2}), X_{i1} - X_{i2}\rangle_0 &= \frac{1}{2}\int_\Omega \partial_t(X_{i1} - X_{i2})^2 \\ &= \frac{1}{2}\partial_t \int_\Omega |X_{i1} - X_{i2}|^2 = \frac{1}{2}\partial_t \|X_{i1} - X_{i2}\|_2^2 .\end{aligned} \tag{3.23}$$

The second term,

$$\langle \nabla(X_{i1} - X_{i2}), \nabla(X_{i1} - X_{i2})\rangle_0 = \|\nabla(X_{i1} - X_{i2})\|_2^2 \geq 0. \tag{3.24}$$

The third term,

$$\begin{aligned}\langle u \cdot \nabla(X_{i1} - X_{i2}), X_{i1} - X_{i2}\rangle_0 &= \frac{1}{2}\int_\Omega u \cdot \nabla(X_{i1} - X_{i2})^2 \\ &= -\frac{1}{2}\int_\Omega (\nabla \cdot u)(X_{i1} - X_{i2})^2 + \frac{1}{2}\int_{\partial\Omega} (\mathbf{n} \cdot u)(X_{i1} - X_{i2})^2 \\ &= \frac{1}{2}\int_{\partial\Omega} (\mathbf{n} \cdot u)(X_{i1} - X_{i2})^2 \geq 0.\end{aligned} \tag{3.25}$$

The last term, we must come back to the definition of $f(X)$ as in (3.20). If $X_i = A$, this term is zero. If X_i is B_s or B_p, then

$$\langle f(X_{i1})X_{i1}, X_{i1} - X_{i2}\rangle_0 - \langle f(X_{i2})X_{i2}, X_{i1} - X_{i2}\rangle_0 = \int_\Omega f(X_{i1})(X_{i1} - X_{i2})^2 \geq 0.$$
$$(\text{Since } f(X_{i1}) = f(X_{i2}))$$

If X_i is S, then

$$\begin{aligned}&\langle f(X_{i1})X_{i1}, X_{i1} - X_{i2}\rangle_0 - \langle f(X_{i2})X_{i2}, X_{i1} - X_{i2}\rangle_0 \\ &= \int_\Omega \frac{B_s}{K_s + S_1} S_1(S_1 - S_2) - \int_\Omega \frac{B_s}{K_s + S_2} S_2(S_1 - S_2) \\ &= \int_\Omega \frac{K_s(S_1 - S_2)^2}{(K_s + S_1)(K_s + S_2)} B_s \geq 0.\end{aligned}$$

[2]Because $X_{i1}, X_{i2} \in L^2(Q_i)$, so $(X_{i1} - X_{i2})(x, y; \cdot) \in Q_i$

Thus, for the last term, we can write in short as

$$\langle f(X_{i1})X_{i1}, X_{i1} - X_{i2}\rangle_0 - \langle f(X_{i2})X_{i2}, X_{i1} - X_{i2}\rangle_0 = \int_\Omega \psi(X_{i1}, X_{i2})(X_{i1} - X_{i2})^2 \geq 0. \tag{3.26}$$

where ψ is defined as

$$\psi(X_{i1}, X_{i2}) = \begin{cases} 0 \quad \text{if } X_i \text{ is } A, \\ f(X_{i1}) \quad \text{if } X_i \text{ is } B_s \text{ or } B_p, \\ \dfrac{K_s B_s}{(K_s + S_1)(K_s + S_2)} \quad \text{if } X_i \text{ is } S. \end{cases}$$

Substitute (3.23), (3.24), (3.25), (3.26) into (3.22), we get:

$$\frac{1}{2}\partial_t \|X_{i1} - X_{i2}\|_2^2 + \frac{1}{2}\int_{\partial\Omega} (\mathbf{n}\cdot u)(X_{i1} - X_{i2})^2 + \|\nabla(X_{i1} - X_{i2})\|_2^2 + \int_\Omega \psi(X_{i1}, X_{i2})(X_{i1} - X_{i2})^2 = 0 \tag{3.27}$$

Therefore,

$$\partial_t \|X_{i1} - X_{i2}\|_2^2 \leq 0.$$

Take the integral from 0 to t with $t \geq 0$, we have

$$\int_0^t \partial_t \|X_{i1} - X_{i2}\|_2^2 \leq 0,$$

this yields,

$$\|(X_{i1} - X_{i2})(\cdot, t)\|_2^2 \leq \|(X_{i1} - X_{i2})(\cdot, 0)\|_2^2 \qquad \forall t \geq 0.$$

On the other hand $(X_{i1} - X_{i2})(\cdot, 0) = 0$ since both X_{i1} and X_{i2} satisfy the initial conditions (3.17), so:

$$\|(X_{i1} - X_{i2})(\cdot, t)\|_2^2 \leq 0 \quad \forall t \geq 0,$$

which means that $\|(X_{i1} - X_{i2})(\cdot, t)\|_2^2 = 0, \forall t \geq 0$. Combine this with assumption $\mathbf{n}\cdot u \geq 0$ then (3.27) becomes

$$\begin{aligned} 0 &\geq \|\nabla(X_{i1} - X_{i2})\|_2^2 + \int_\Omega \psi(X_{i1}, X_{i2})(X_{i1} - X_{i2})^2 \\ &\geq \|\nabla(X_{i1} - X_{i2})\|_2^2 + C_1\|X_{i1} - X_{i2}\|_2^2 \quad (C = \inf\{\psi(X_{i1}, X_{i2})\} \geq 0) \\ &\geq C_2(\|\nabla(X_{i1} - X_{i2})\|_2^2 + \|X_{i1} - X_{i2}\|_2^2) \quad (C_2 = \sup\{1, C_1\}) \\ &= C_2 \|X_{i1} - X_{i2}\|_{G_i}^2 \end{aligned}$$

In conclusion, $X_{i1} = X_{i2}$ in $L^2(G_i)$ or our main problem has unique solution.

Chapter 4

Numerical results

4.1 Parameters

Table (4.1) lists the parameters and values which are used in our simulations. We will test with many values of parameters whose source name are "Estimated" to find an optimal antimicrobial dosing strategy.

Parameter	**Symbol**	**Units**	**Value**	**Source**
Maximum Specific Growth Rate	μ	h^{-1}	0.417	[12]
Yield Coefficient	Y		0.2	[12]
Monod Coefficient	K_s	mg l^{-1}	0.2	[12]
Maximum Disinfection Rate	k_d	h^{-1}	40	Estimated
Rate of Loss	k_l	h^{-1}	0.001	Estimated
Rate of Gain	k_g	h^{-1}	0.05	Estimated
Substrate Influent Concentration	C_s	mg l^{-1}	8	Estimated,[12]
Antimicrobial Influent Concentration	C_a	mg l^{-1}	5	Estimated,[12]
Neutralizer reaction rate coefficient	k_r	$m^3g^{-1}h^{-1}$	10	[6]
Reactive antimicrobial agent	N		0.4	Assumed in [6]
Nutrient diffusion coefficient	D_s	m^2h^{-1}	9.67×10^{-6}	[12]
Antimicrobial diffusion coefficient	D_a	m^2h^{-1}	1.80×10^{-6}	[12]
Velocity	u	mh^{-1}		Estimated
Initial condition for susceptible cells	B_s^0		500	Estimated
Initial condition for persister cells	B_p^0		0	Estimated

Table 4.1: Parameters used in the simulations.

4.2 Convection-Dominated problems

Why do we consider this kind of problem? Because my main simulation will use some real parameters from experimental researches of Cogan and Stewart [6, 12] (cf. Table 4.1). There are some of them which are extremely small give bad effects to the final result of our problem. Specifically, the convection-dominated problem occurs. This is the reason why I attach this section about convection-dominated problem into my report.

4.2.1 The problem

Consider problems (2.1) and (2.8). These application specific equations often share the property that their so-called *global Péclet number* [10]:

$$\mathrm{Pe} := \frac{\|c\|_\infty \mathrm{diam}(\Omega)}{\|D\|_\infty}.$$

Convection-dominance just means in (2.1), (2.8):

$$D \ll \|\vec{b}\|.$$

The diffusion term is very small relative to the convection term or Péclet number is significantly larger than one.

Let's consider some examples to have more understanding about this problem.

Example 1. (One dimensional) Given a constant diffusion coefficient $k > 0$, consider the boundary value problem

$$\begin{aligned} (-ku' + u)' &= 0 \quad \text{in } \Omega := (0,1), \\ u(0) = u(1) - 1 &= 0. \end{aligned}$$

Its solution is

$$u(x) = \frac{1 - \exp(x/k)}{1 - \exp(1/k)}.$$

Given an equidistant grid of width $h = 1/(M+1), M \in \mathbb{N}$. Using finite different method, we have the difference equation:

$$\begin{aligned} -k\frac{u_{i-1} - 2u_i + u_{i+1}}{h^2} + \frac{u_{i+1} - u_{i-1}}{2h} &= 0, \quad i \in \{1, ..., M\} =: \Lambda, \\ u_0 = u_{M+1} - 1 &= 0. \end{aligned}$$

Collecting the coefficients and multiplying the result by $2h$, we arrive at

$$\left(\frac{-2k}{h} - 1\right) + \frac{4k}{h}u_i + \left(-\frac{2k}{h} + 1\right)u_{i+1} = 0, \quad i \in \Lambda.$$

If we make the ansatz $u_i = \lambda^i$ then the difference equations can be solved exactly:

$$u_i = \frac{1 - \left(\frac{2k+h}{2k-h}\right)^i}{1 - \left(\frac{2k+h}{2k-h}\right)^{M+1}}.$$

In the case $2k < h$, the numerical solution considerably oscillates, in contrast to the behaviour of the exact solution u (see Figure 4.1). These oscillations do not disappear until $h < 2k$ is reached (see Figure 4.2).

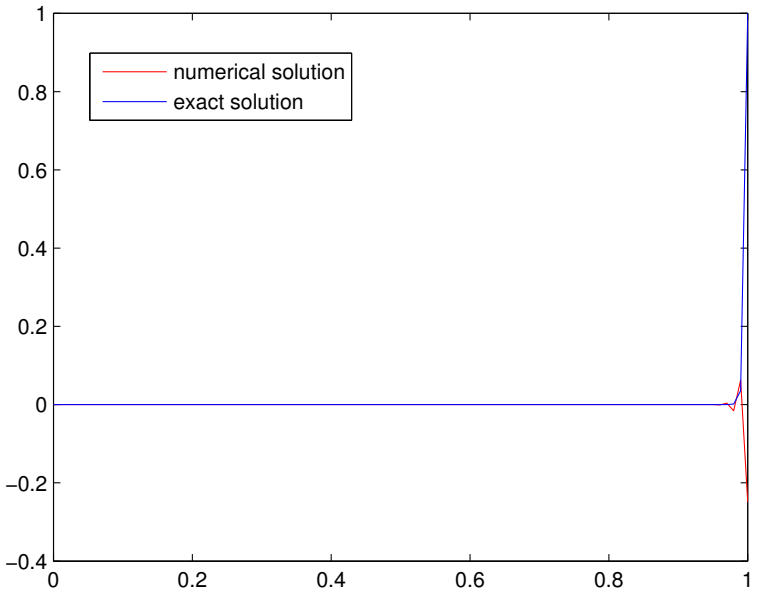

Figure 4.1: Solution for $k = 0.003, M = 100, h = 1/M = 0.01$, $(2k < h)$. The Péclet number $\mathrm{Pe} = 1000/3 \gg 1$. The oscillations occurs.

Example 2. (Two dimensional) Consider the problem

$$\begin{aligned} -\varepsilon\Delta u + c \cdot \nabla u + ru &= f \quad \text{in } \Omega = [0,1] \times [0,1], \\ u &= 0 \quad \text{on } \partial\Omega. \end{aligned}$$

where $c = (0,1)^T, r = 1$ and f will be calculated such that the given exact solution

$$u(x,y) = 0.5[\sin(\pi x).\sin(\pi y).(1 - \tanh((0.5 - x)/0.05))]$$

By Matlab, we can calculate the function f:

$$\begin{aligned} f = \frac{1}{2}(&\sin(\pi y)(\tanh(20x-10)+1)(21\sin(\pi x) + \pi\cos(\pi x) - 20\sin(\pi x)\tanh(20x-10) \\ &+ 800\varepsilon\sin(\pi x)\tanh(20x-10) + 2\pi^2\varepsilon\sin(\pi x) - 800\varepsilon\sin(\pi x)\tanh(20x-10)^2 \\ &- 40\pi\varepsilon\cos(\pi x) + 40\pi\varepsilon\cos(\pi x)\tanh(20x-10))); \end{aligned}$$

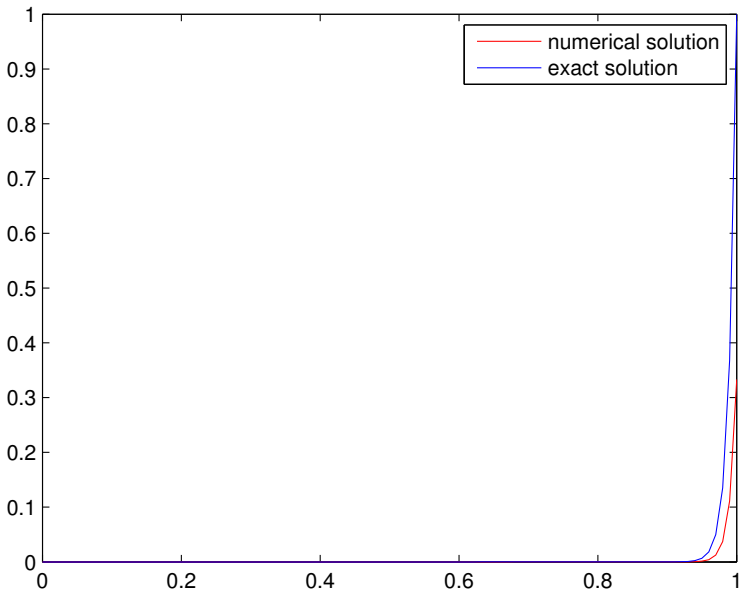

Figure 4.2: Solution for $k = 0.01, M = 100, h = 1/M = 0.01$, $(2k > h)$. The Péclet number $\mathrm{Pe} = 100$. The oscillations do not occur.

Using FreeFEM++ (cf. [1]), we can plot the exact solution as in Figure 4.3 and the numerical solution by Standard Galerkin Method as in Figure 4.4. We will consider the error estimate and convergence rate of these solution in next section.

4.2.2 The Streamline Diffusion Method

Unfortunately, the finite element method mentioned before fails when applied to convection dominated equations. This is explained that the theoretical results are still true for this kind of problem but some assumptions of statements therein (such as "for sufficiently small h") lack sharpness. This, in turn, may lead to practically unrealistic conditions. Specifically, in our problem, those are parameters in Table 4.1.

There are many methods to solve convection-dominated problem. Here we will use the Streamline-Diffusion Method (or SUPG method[1]). The streamline-diffusion method is the prevalent method in the numerical treatment of stationary convection-dominated problems. The basic idea of this method consists in the addition of suitably weighted residuals to the variational formulations (2.3). The results from research of Pavel et al. [2] indicate that it can be applied in time-dependent problem (2.9) with this method.

Because of the assumption $u \in H^{k+1}(\Omega), k \in \mathbb{N}$, the difference equation (2.1) can be interpreted as an equation in $L^2(\Omega)$. In particularly, it is valid on any element $K \in \mathcal{T}_h$ in the

[1]Streamline upwind Petrov Galerkin Method

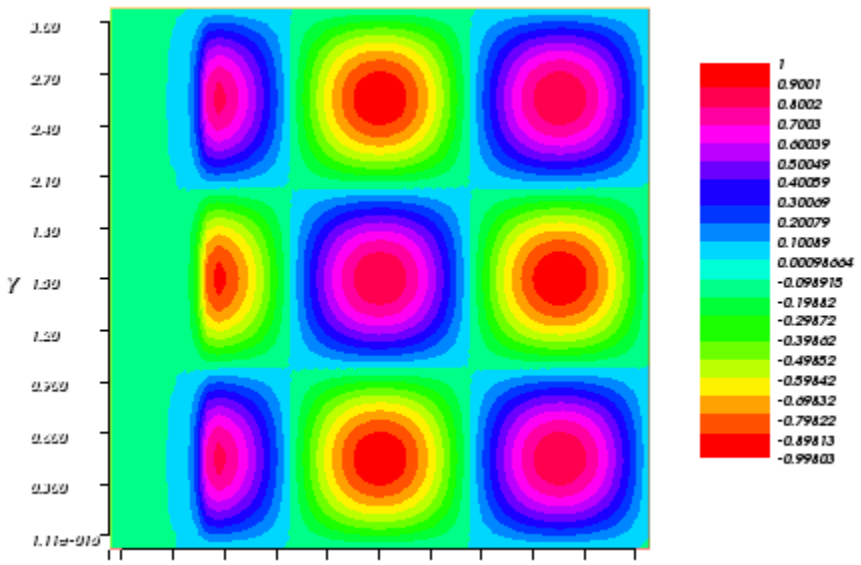

Figure 4.3: Exact solution for $\varepsilon = 9.67 \times 10^{-6}$.

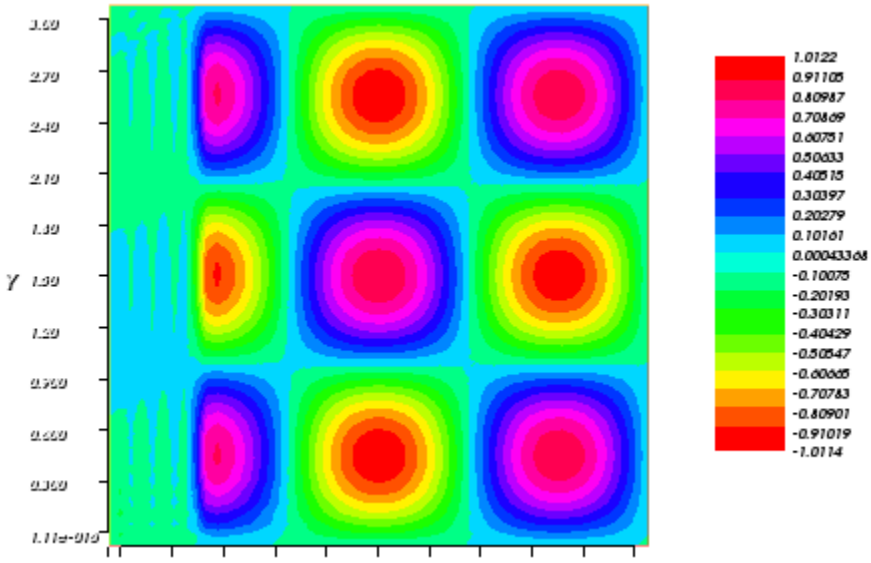

Figure 4.4: Standard Galerkin method for $\varepsilon = 9.67 \times 10^{-6}$. Convection-dominated occurs.

sense of $L^2(K)$, i.e.,

$$-D\Delta u + c \cdot \nabla u + Ru = f \quad \text{a.e. in } K \text{ and for all } K \in \mathcal{T}_h.$$

Next, we take the elementwise defined mapping $\tau : V_h \to L^2(\Omega)$ and multiply the local differential equation in $L^2(\Omega)$ by the restriction of $\tau(v_h)$ to K. Scaling by a parameter $\delta_K \in \mathbb{R}$ and summing the results over all elements $K \in \mathcal{T}_h$, we obtain

$$\sum_{K \in \mathcal{T}_h} \delta_K \left\langle -D\Delta u + c \cdot \nabla u + Ru, \tau(v_h) \right\rangle_{0,K} = \sum_{K \in \mathcal{T}_h} \delta_K \left\langle f, \tau(v_h) \right\rangle_{0,K}.$$

If we add this relation to equation (2.3) restricted to V_h, we see that the weak solution $u \in V \cap H^{k+1}(\Omega)$ satisfies the following variational equation:

$$a_h(u, v_h) = \langle f, v_h \rangle_h \quad \forall v_h \in V_h,$$

where

$$\begin{aligned} a_h(u, v_h) &:= a(u, v_h) + \sum_{K \in \mathcal{T}_h} \delta_K \left\langle -D\Delta u + c \cdot \nabla u + Ru, \tau(v_h) \right\rangle_{0,K}, \\ \langle f, v_h \rangle_h &:= \langle f, v_h \rangle_0 + \sum_{K \in \mathcal{T}_h} \delta_K \left\langle f, \tau(v_h) \right\rangle_{0,K}. \end{aligned}$$

with a is defined in (2.2).

Then the corresponding descretization reads as follows: Find $u_h \in V_h$ such that

$$a_h(u_h, v_h) = \langle f, v_h \rangle_h \quad \forall v_h \in V_h. \tag{4.1}$$

The mapping τ (weighting operator) can be chosen as

- Streamline upwind weight operator: $\tau(v_h) := c \cdot \nabla v_h$.
- Galerkin/least squares operator: $\tau(v_h) := -D\Delta v_h + c \cdot \nabla v_h + Rv_h$. In this case, we note that $\Delta v_h|_K = 0$ for all $K \in \mathcal{T}_h$.

Disadvantage of this method is choosing an appropriate parameter δ_K, it is chosen more or less empirically. This is really a problem when SUPG method is embedded into more complex programs, our main problem is an example.

4.2.3 Analysis of the SUPG method

In this section, we will list some important results (without proof) from [10] about streamline diffusion method.

Corollary 1. Suppose the problems (2.1) and (4.1) have a solution $u \in V \cap H^{k+1}(\Omega)$ and $u_h \in V_h$, respectively. Then the following error equation is valid:

$$a_h(u - u_h, v_h) = 0 \quad \text{for all } v_h \in V_h.$$

From Theorem 3.43 of [10], a so-called *inverse inequality* can be proven

$$\|\Delta v_h\|_{0,K} \leq \frac{c_{inv}}{h_K}|v_h|_{1,K} \tag{4.2}$$

with $c_{inv} > 0$ for all $v_h \in V_h$ and all $K \in \mathcal{T}_h$.

The choice of δ_K is satisfied

$$0 < \delta_K \leq \frac{1}{2}\min\left\{\frac{h_K^2}{Dc_{inv}^2}, \frac{r_0}{\|r\|_{0,\infty,K}^2}\right\} \tag{4.3}$$

where $r_0 > 0$ is a constant such that the inequality $r - \frac{1}{2}\nabla \cdot c \geq r_0$ is valid in Ω

A so-called *streamline-diffusion norm* is also defined by

$$\|v\|_{sd} := \left\{D|v|_1^2 + r_0\|v\|_0^2 + \sum_{K\in\mathcal{T}_h}\delta_K\|c\cdot\nabla v\|_{0,K}^2\right\}^{\frac{1}{2}}, \qquad v \in V.$$

The error estimate is determined through following theorem

Theorem 6. Let parameter δ_K is chosen such that the condition 4.3. If the weak solution u of 2.1 belongs to $H^{k+1}(\Omega)$ then

$$\|u - u_h\|_{sd} \leq C(\sqrt{D} + \sqrt{h})h^k|u|_{k+1}$$

Proof. See the proof of Theorem 9.3 in [10]. □

Example 3. Come back to Example 2 using Streamline-diffusion method with many values of ε, we compute the error estimate $\|u - u_h\|_{sd}$ (under sd-norm) and convergence order (under Theorem 6) in order that we can understand the effect of SUPG method compared with standard Galerkin method.

Choose $r_0 = 0.5$, we have the following tables 4.2, 4.3, 4.4. We can see that when $\varepsilon = 0.1$, the convection-dominated doesn't occur, the Standard Galerkin method is more accuracy than the other one with convergence order is approximately 2 with h is sufficiently small. With bigger ε in Table 4.3 and Table 4.4, the problem occurs and the SUPG method is more accuracy with convergence order is bigger alongside with smaller error estimate.

h_K	Streamline method		Standard method	
	$\|u-u_h\|_{sd}$	Convergence order	$\|u-u_h\|_1$	Convergence order
0.7071	1.16172	—	0.8556	—
0.3536	0.881091	0.3989	0.8433	0.0208
0.1768	0.613169	0.523	0.4019	1.0694
0.0884	0.313783	0.9665	0.112	1.8433
0.0442	0.116256	1.4325	0.0262	2.0962
0.0221	0.0368874	1.6561	0.0067	1.9762
0.011	0.010372	1.8304	0.0017	1.9933
0.0055	0.00274841	1.916	0.0004	1.9983
0.0028	0.00070729	1.9582	0.0001	1.9996

Table 4.2: Table of error estimate and convergence rate between SUPG method and Standard Galerkin method. Test with $\varepsilon = 0.1$.

h_K	Streamline method		Standard method	
	$\|u-u_h\|_{sd}$	Convergence order	$\|u-u_h\|_1$	Convergence order
0.7071	0.165949	—	3.1255	—
0.3536	0.132962	0.3197	2.9767	0.0703
0.1768	0.0560095	1.2473	1.9841	0.5853
0.0884	0.0474627	0.2389	0.5815	1.7706
0.0442	0.0338107	0.4893	0.0947	2.6181
0.0221	0.0169572	0.9956	0.0219	2.1126
0.011	0.0064275	1.3996	0.0054	2.022
0.0055	0.00208483	1.6243	0.0013	2.0053
0.0028	0.00061887	1.7522	0.0003	2.0013

Table 4.3: Table of error estimate and convergence rate between SUPG method and Standard Galerkin method. Test with $\varepsilon = 0.01$.

h_K	Streamline method		Standard method	
	$\|u-u_h\|_{sd}$	Convergence order	$\|u-u_h\|_1$	Convergence order
0.7071	0.0326477	—	4.1708	—
0.3536	0.177947	-2.446	4.8313	-0.212
0.1768	0.0954576	0.8985	5.3715	-0.153
0.0884	0.0337185	1.5013	2.6251	1.0329
0.0442	0.0093365	1.8526	0.2004	3.7111
0.0221	0.00231162	2.014	0.0262	2.9341
0.011	0.0004453	2.3761	0.0065	2.014
0.0055	6.42E-05	2.7941	0.0016	2.0006
0.0028	4.50E-06	3.8359	0.0004	1.9996

Table 4.4: Table of error estimate and convergence rate between SUPG method and Standard Galerkin method. Test with $\varepsilon = 1 \times 10^{-4}$.

4.3 Special cases

In this section, we will explore some special cases of our main problem. We will use the SUPG method with

$$\delta_K = \left(\frac{1}{h_K} + \frac{\tau_n \varepsilon}{h_K^2} \right)^{-1}$$

Remark: Because of time discretization, at the specific time τ_n, the time-dependent problem will be considered as the stable problem. So we can use the SUPG method as in the stability case. That is the reason why in the δ_K formula, there is the presence of τ_n.

4.3.1 Test case with B_s, no B_p, no A

Because there is no A, B_s is not dead or the term *disinfection* in susceptible equation 3.7 will be eliminated. And also because of no B_p, so there is not any B_s converting to B_p and there is no B_p reverting back to the B_s. Those are the reasons why in B_s equation 3.7, these terms *lost* and *reversion* are eliminated. Finally, we have the equation of B_s:

$$\frac{\partial B_s}{\partial t} + u \cdot \nabla B_s - \hat{k_s}(S) B_s = 0,$$

Clearly from above equation, we can see that B_s will always increase without decreasing. It is verified by the test with FreeFem++ (See Figure 4.5, 4.6). Because of the advection term, the concentration of B_s moves from left to right, so the concentration at the left will decrease after a period of time, we can see that at Figure 4.7. In Freefem++ test, with time greater than 1.3, the oscillation occurs. It maybe comes from CFL condition.

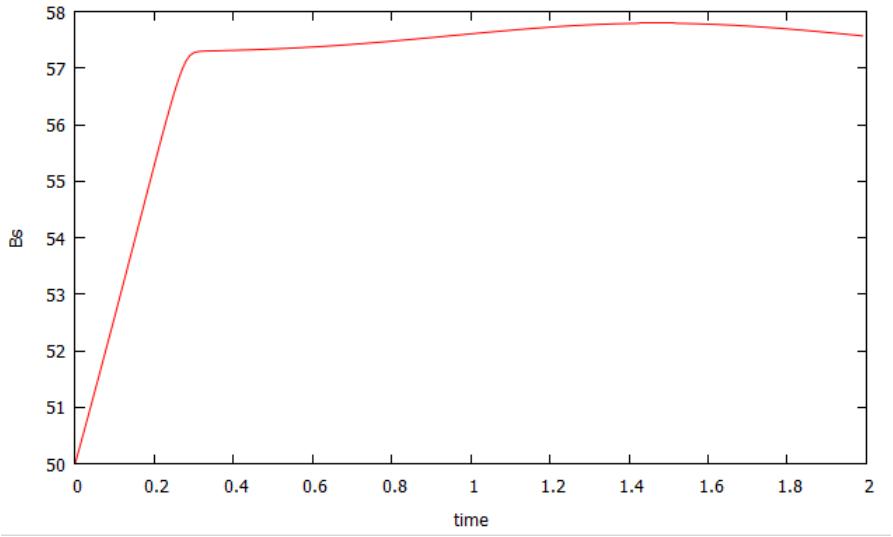

Figure 4.5: Concentration of B_s. Test with B_s, no B_p and no A. Gnuplot at point $(0.5; 0.05)$ inside biofilm region.

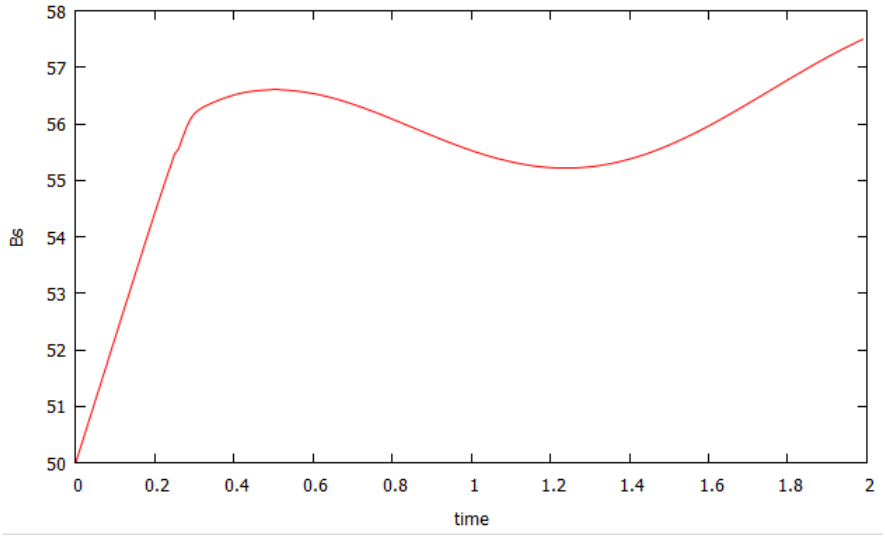

Figure 4.6: Concentration of B_s. Test with B_s, no B_p and no A. Gnuplot at point $(0.65; 0.05)$ inside biofilm region.

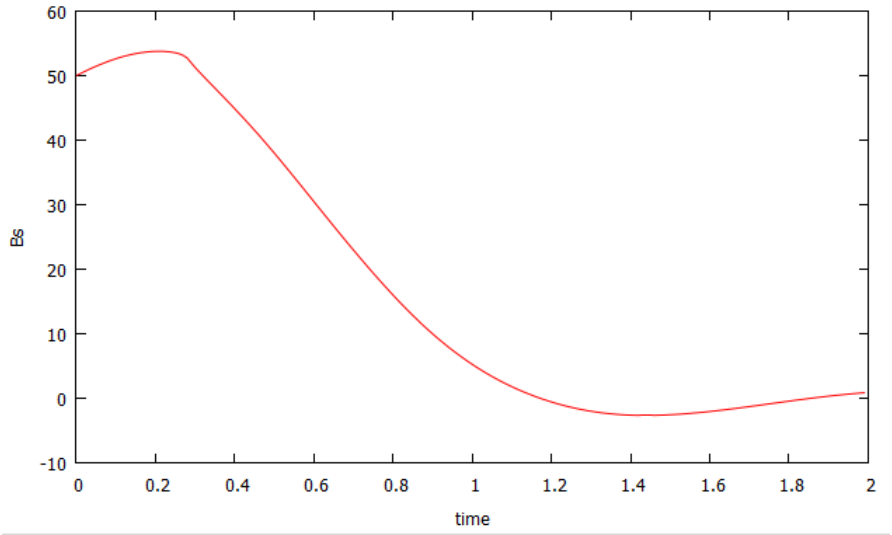

Figure 4.7: Concentration of B_s. Test with B_s, no B_p and no A. Gnuplot at point $(0.3; 0.05)$ inside biofilm region.

4.3.2 Test with B_s and A, no B_p

When B_p absents, these terms *loss* and *reversion* also absent from B_s equation with the same reason as the previous test. Difference from the previous test case, in this case, with the presence of A, B_s start to decrease. I have tested with many values of A, the bigger A, the faster decreasing B_s. However, A is consumed by B_s and reacts with Neutralizing agent so after a short time, A is go down to zero (see Figure 4.8) and B_s begin to increase again (see Figure 4.9).

Notice that the results are different at different points. we have tested with many arbitrary points. Here, we choose the typical points to present.

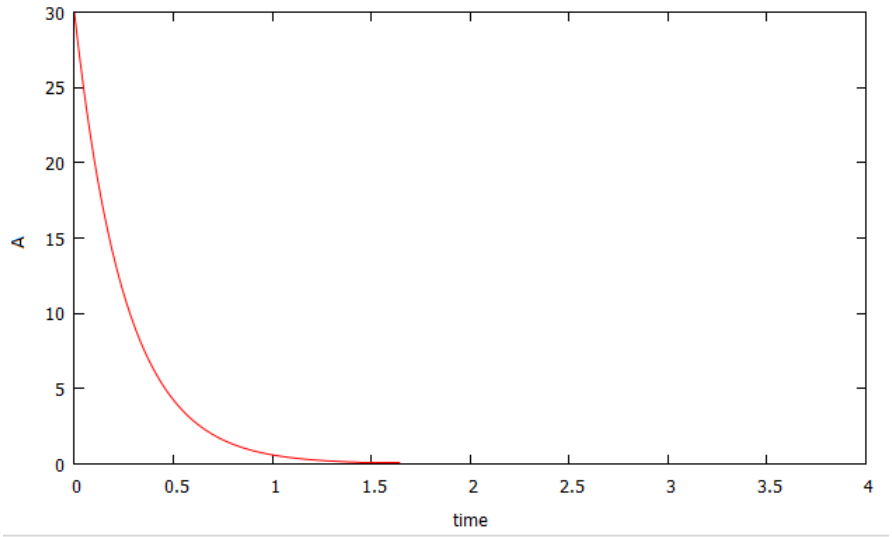

Figure 4.8: Concentration of A. Test with B_s, A, no B_p. Initial $A = 30$. Gnuplot at point $(0.5; 0.05)$ inside biofilm region.

4.3.3 Test with full B_s, B_p and A in scheme

B_s decreases because it is killed by A and converts to B_p without gaining from reversion of B_p. It comes from our assumption that if A is available then B_p will not convert to B_s. When A decreases from consumption of B_s and reaction with neutralizing agent (see Figure 4.10), B_s starts to increase (see Figure 4.11). B_p always increase because they do not reverse back to B_s (since $k_g = 0$ or A is always available). I think that with this assumption, we will not never kill these persister cells (which is always increase). So the dosing is not successful. (see Figure 4.12).

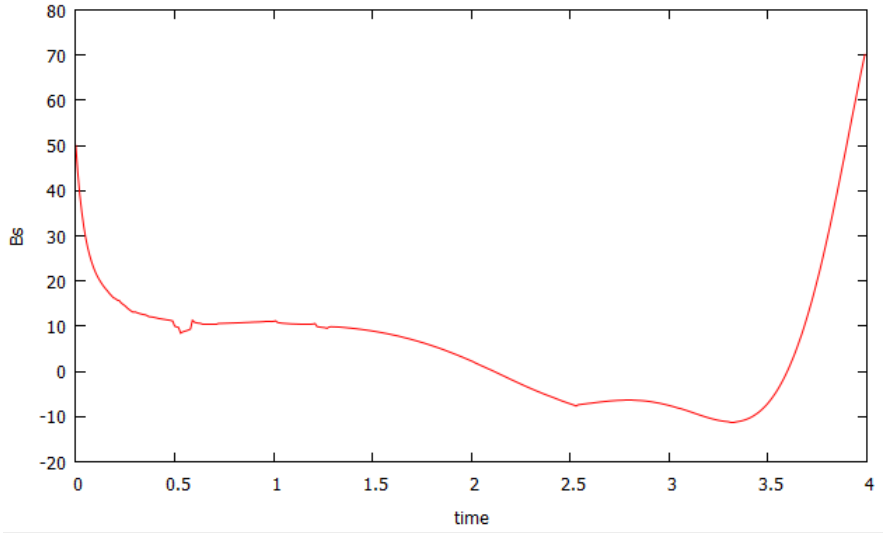

Figure 4.9: Concentration of B_s. Test with B_s, A, no B_p. Initial $A = 15$. Gnuplot at point $(0.5; 0.05)$ inside biofilm region.

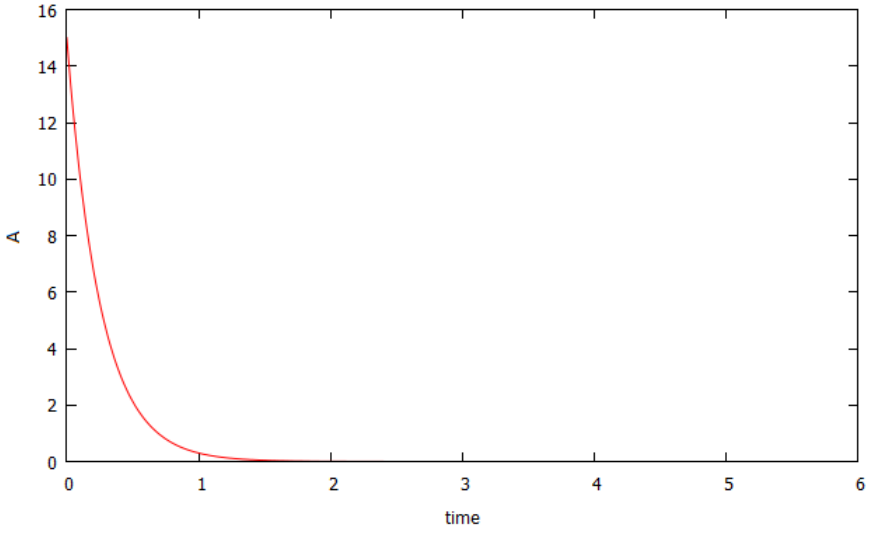

Figure 4.10: Concentration of A. Test with B_s, A and B_p. Initial $A = 15$. Gnuplot at point $(0.5; 0.05)$ inside biofilm region.

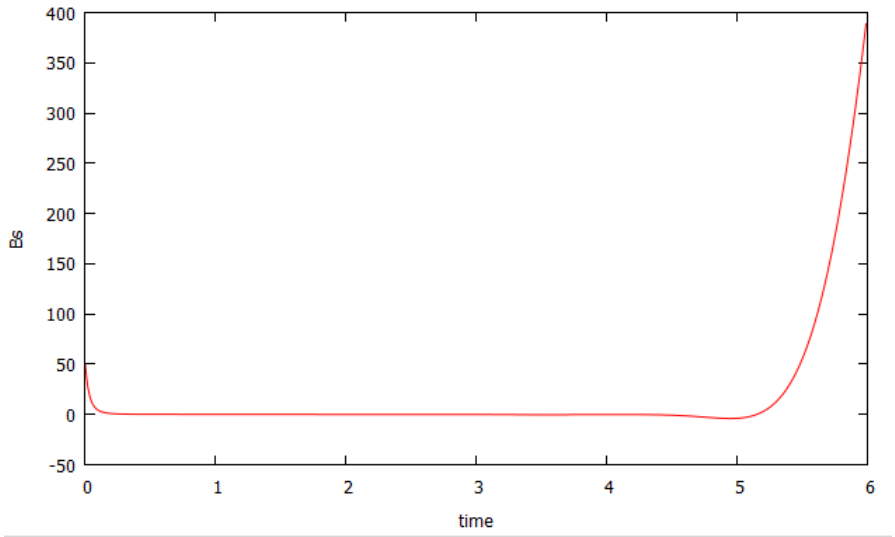

Figure 4.11: Concentration of B_s. Test with B_s, A and B_p. Initial $A = 15$. Gnuplot at point $(0.5; 0.05)$ inside biofilm region.

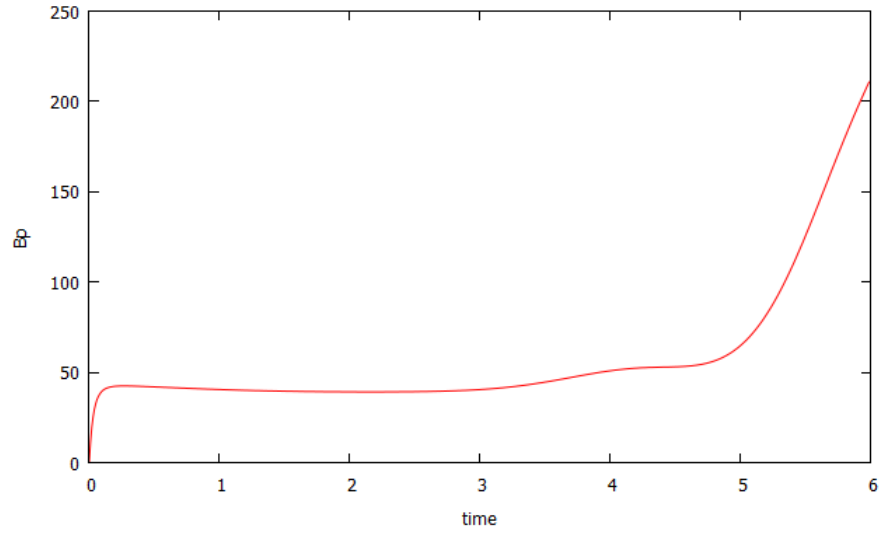

Figure 4.12: Concentration of B_p. Test with B_s, A and B_p. Initial $A = 15$. Gnuplot at point $(0.5; 0.05)$ inside biofilm region.

Chapter 5

Conclusion

In conclusion, the report mainly focus on using the Finite Element Method and simulation analysis in order to explore biofilm resistance to antimicrobial agents via a system of 4 PDE equations. With experimental assumptions from documents of Cogan and Stewart, report considered some special cases of the main problem.

Besides that, due to convection-dominated problems and the limitation in passively using data from a third party, the report has not reach the final results as our wishes. However, with the best effort, it has showed some specific cases and given practical comments (cf. Chapter 4).

In terms of future development, firstly we hope to resolve the remaining problems, which propose a strategy for optimizing the antimicrobial dosing. Second, the considered PDE systems is assumed linear, this is not true from reality because it may be a nonlinear one. Third, we want to derive posterior error estimators allowing to generate adaptive meshes, thus reduce the computational cost, and to detect accurately the free boundary. Finally, it need to be noticed about the resistance of bateria to antimicrobial agents. In other words, the bacteria may reformat to be a stronger form to resist antimicrobial agents.

Appendix A

Finite Element & FreeFEM software

A.1 Finite Elements (FE)

This section of the appendix give more fundamental information about finite elements.

A.1.1 Definition of Finite Element

Following Ciarlet, a finite element is defined as a triplet $\{K, P, \Sigma\}$,

Definition 6. A finite element consists of a triplet $\{K, P, \Sigma\}$ where:

(i) K is a compact, connected, Lipschitz subset of $\mathbb{R}^d$ with non-empty interior.

(ii) P is a vector space of functions $p : K \to \mathbb{R}^m$ for some positive integer m (typically $m = 1$ or d).

(iii) Σ is a set of n_{sh} linear form $\{\sigma_1, ..., \sigma_{n_{sh}}\}$ acting on the elements of P, and such that the linear mapping

$$P \ni p \mapsto (\sigma_1(p), ..., \sigma_{n_{sh}}(p)) \in \mathbb{R}^{n_{sh}},$$

by bijective, i.e., Σ is a basis for $\mathcal{L}(P; \mathbb{R})$. The linear forms $\{\sigma_1, ..., \sigma_{n_{sh}}\}$ are called the local degrees of freedom.

A.1.2 Some typical finite elements

The purpose of this section is to give some examples of finite elements (FE) in two and three dimensional. Here is just a list of names of them, more details can be found at section 1.2 of [9] or section 3.2 of [3].

- Lagrange FE,
- Tensor product Lagrange FE,

- Prismatic Lagrange FE,
- The Crouzeix-Raviart FE,
- The Raviart-Thomas FE,
- The Nédélec (or edge) FE.

A.1.3 Triangulations of space

The construction of conforming finite element spaces is based on a suitable partition of the computational domain.

Definition 7. Let $\mathcal{T}_h$ be a partition of Ω into closed triangles K (i.e., including the boundary ∂K) with the following properties:

(i) $\overline{\Omega} = \cup_{K \in \mathcal{T}_h} K$

(ii) For $K, K' \in \mathcal{T}_h, K \neq K'$,
$$\text{int}(K) \cap \text{int}(K') = \emptyset,$$
where $\text{int}(K)$ denotes the open triangle (without boundary ∂K)

(iii) If $K \neq K'$ but $K \cap K' \neq \emptyset$, then $K \cap K'$ is either a point or common edge of K and K'

A partition of Ω with the properties (i) , (ii) is called a *triangulation* of Ω. If, in addition, a partition of Ω satisfies property (iii), it is called a *conforming triangulation.*

In other words, a triangulation of a polygonal domain Ω is a subdivision consisting of triangles having the property that "no vertex of any triangle lies in the interior of an edge of another triangle" (cf. [3]).

The vertices of triangles are called the *nodes.*

The triangles of a triangulation will be numbered $K_1, ..., K_N$. The subscript h indicates the fineness of the triangulation, e.g.,
$$h := \max\{\text{diam}(K) | K \in \mathcal{T}_h\},$$
where $\text{diam}(K) := \sup\{|x-y|\colon x, y \in K\}$ denotes the diameter of K. Thus h is the maximum length of the edges of all the triangles. Sometimes, $K \in \mathcal{T}_h$ is also called a (geometric) *element* of the partition.

The Ritz-Galerkin method in section 2.2.3 to approximate the solution u by u_h in space V_h is obtained by building the ansatz space V_h (with given triangulation $\mathcal{T}_h$ of Ω) is defined as follows
$$V_h := \{v \in H^1(\Omega) : v|K \in \mathcal{P}^k(K), v|_{\partial\Omega} = 0, \forall K \in \mathcal{T}\}, \tag{A.1}$$
where $\mathcal{P}^k(K)$ is the space of polynomials of degree at most k supported in K.

We write $X_h = X_h(\Omega, \mathcal{T}_h, V_h)$ and call it *the finite element space.* We shall usually use X_h meaning V_h.

A.1.4 The Interpolant

Definition 8. (Local interpolant) Given a finite element $(K, \mathcal{P}, \mathcal{N})$, let the set $\{\phi_i : 1 \leq i \leq k\} \subseteq \mathcal{P}$ be the basis dual to $\mathcal{N}$. If v is a function for which all $N_i \in \mathcal{N}, i = 1, ..., k$, are defined, then we define the *local interpolant* by

$$\mathcal{I}_K v := \sum_{i=1}^{k} N_i(v)\phi_i.$$

See more details and examples in section 3.1 of [3].

Definition 9. (Global interpolant) Suppose Ω is a domain with a subdivision $\mathcal{T}$. Assume each element domain, K, in the subdivision is equipped with some type of shape functions, $\mathcal{P}$, and nodal variables, $\mathcal{N}$, such that $(K, \mathcal{P}, \mathcal{N})$ forms a finite element. Let m be the order of the highest partial derivatives involved in the nodal variables. For $f \in C^m(\overline{\Omega})$, the *global interpolant* is defined by

$$\mathcal{I}_{\mathcal{T}} f|_{K_i} = \mathcal{I}_{K_i} f,$$

for all $K_i \in \mathcal{T}$. (cf. [3])

A.2 FreeFEM++ software

This section introduces some points about the FreeFEM++. More and all necessary information are available in FreeFEM++ document, cf. [1]. FreeFEM++ is a free software to solve PDE using the Finite Element Method. It runs on many platform as Windows, Linux and MacOS. It can help us do many thing: mesh generation, automatic building of mass/rigid matrices and second member, diverse linear solvers integrated, works for 2D or 3D problems, generates graphic/text/file outputs, and a lot more...

Bibliography

[1] *Freefem++, finite element software*. http://www.freefem.org/ff++/.

[2] P. B. Bochev, M. D. Gunzburger, and J. N. Shadid, *Stability of the supg finite element method for transient advection–diffusion problems*, Computer methods in applied mechanics and engineering, 193 (2004), pp. 2301–2323.

[3] S. C.Brenner and L. Scott, *The Mathematical Theory of Finite Element Methods*, vol. 15 of Texts in Applied Mathematics, Springer, New York, third ed., 1994.

[4] N. Cogan, *Effects of persister formation on bacterial response to dosing*. http://www.math.fsu.edu/~cogan/research/papers/.

[5] ——, *Two-fluid model of biofilm disinfection*, 70 (2008), pp. 800–819.

[6] N. Cogan, R. Cortez, and L. Fauci, *Modeling physiological resistance in bacterial biofilms*, Bulletin of Mathematical Biology, 67 (2005), pp. 831–853.

[7] A. B. Cunningham, J. E. Lennox, and R. J. Ross, *Biofilms: The hypertextbook*, 2010. http://www.cs.montana.edu/webworks/projects/stevesbook/index.html.

[8] C. Dreszer, S. Sperling, and M. Tavian, *Biofilms in medicine*.

[9] A. Ern and J.-L. Guermond, *Theory and Practice of Finite Elements*, vol. 159 of Applied Mathematical Sciences, Springer, New York, 2004.

[10] P. Knabner and L. Angermann, *Numerical Methods for Elliptic and Parabolic Partial Differential Equations*, vol. 44 of Texts in Applied Mathematics, Springer, New York, 2003.

[11] G. O'Toole, H. B. Kaplan, and R. Kolter, *Biofilm formation as microbial development*, Annual Review of Microbiology, 54 (2000), pp. 49–79.

[12] M. E. Roberts and P. S. Stewart, *Modelling protection from antimicrobial agents in biofilms through the formation of persister cells*, Microbiology, 151 (2005), pp. 75–80.

[13] O. Wanner, *Mathematical Modeling of Biofilms*, IWA Publishing, London, 2006.